Appendix D

Supplementary Information for Chapter 5

.

D.1 General procedures

General Considerations: All manipulations of inorganic complexes were carried out using standard Schlenk or glovebox techniques under an N_2 or Ar atmosphere. Unless otherwise noted, solvents were deoxygenated and dried by thoroughly sparging with N_2 gas followed by passage through an activated alumina column in a solvent purification system (SG Water, USA LLC). For electrochemical measurements under an Ar atmosphere, solvents were further degassed and then stored under Ar. All solvents were stored over activated 3 or 4 Å molecular sieves prior to use. Anhydrous ammonia gas was dried by passage through a calcium oxide drying tube. All reagents were purchased from commercial vendors and used without further purification unless otherwise stated. Tris(2-pyridylmethyl)amine (TPA),[1] tris(2-pyridylmethylamine) iron(II) triflate bis-acetonitrile ([(TPA)Fe(MeCN)$_2$]OTf$_2$),[2] 6-(1,1-di(pyridin-2-yl)ethyl)-2,2'-bipyridine (BPM),[3] 6-(1,1-di(pyridin-2-yl)ethyl)-2,2'-bipyridine iron(II) triflate bis-acetonitrile ([(BPM)Fe(MeCN)$_2$]OTf$_2$),[4] bis(4-(dimethylamino)pyridin-2-yl)methanone,[5] tris(4-(dimethylamino)-2-picolyl)amine (TPA^{NMe2}),[6] tris(4-methoxy-2-picolyl)amine (TPA^{OMe}),[6] 4-(trifluoromethyl)pyridine-2-carboxaldehyde,[7] 4-(trifluoromethyl)-2-ethylpyridine,[8] bis(4-(dimethylamino)pyridin-2-yl)methanone,[9] and methylenetriphenylphosphorane[10] were synthesized according to literature procedures.

Electrochemistry: Voltammetry experiments were carried out with a Biologic VSP-300 or CH Instruments 600B potentiostat using a one-compartment three-electrode cell, and coulometry experiments were carried out with a Biologic VSP-300 potentiostat using a one-compartment three-electrode cell with a septum capped 14/20 joint for headspace analysis.

For voltammetry, a boron-doped diamond (BDD) working electrode (3 mm diameter), a Pt wire counter electrode, and an Ag/AgOTf reference electrode (5 mM AgOTf and 0.1 M $TBAPF_6$ in MeCN) were employed. For controlled potential coulometry (CPC), the same reference electrode was used, but a BDD plate (geometric area: 4 cm^2) and a Pt mesh were used as working and counter electrodes, respectively. All redox potentials in the present work are reported versus the Fc/Fc^+ couple, measured before each experiment to be approximately +0.12 V versus the Ag/AgOTf reference electrode.

Cyclic voltammograms (CVs) were collected at 100 $mV \cdot s^{-1}$ unless otherwise specified. $E_{1/2}$ values for the reversible waves were obtained from the half potential between the oxidative and reductive peaks. CV measurements were performed applying IR compensation, compensating 85% of the resistance measured at one high frequency value (100 kHz).

Gas Chromatography: Gas chromatography was performed in the Caltech Environmental Analysis Center using HP 5890 Series II instruments. Gas quantification was performed with a molecular sieve column attached to a thermal conductivity detector using argon as the carrier gas. Standard curves were generated by direct injection of hydrogen or nitrogen gas. Quantification of background nitrogen was determined using the background oxygen signal. Isotopic measurements were performed with a separate HP 5890 Series II instrument equipped with a GasPro column using helium as the carrier gas.

NMR: NMR spectroscopy was performed using Varian and Bruker 400 MHz NMR spectrometers equipped with broadband auto-tune probes. ^1H NMR chemical shifts are reported in ppm relative to tetramethylsilane, using residual solvent resonances as internal standards.

UV-Vis: Spectra were collected using a Cary 60 instrument with Cary WinUV software.

X-ray Crystallography: XRD studies were carried out at the Caltech Beckman Institute Crystallography Facility on a Bruker D8 Venture diffractometer (Cu Kα radiation). The crystals were mounted on a glass fiber under Paratone N oil. Structures were solved using direct methods with SHELXS or SHELXT and refined against F^2 on all data by full-matrix least squares with SHELXL.[11] All of the solutions were performed in the Olex2 program.[12]

D.2 Synthetic procedures

TPA derivatives

TPA^{CF3} (tris(4-(trifluoromethyl)-2-picolyl)amine)

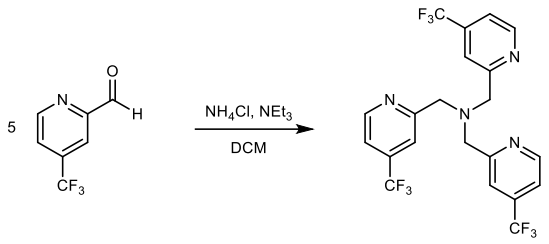

Ammonium chloride (15 mg, 1 eq), 4-(trifluoromethyl)-pyridine-2-carbaldehyde (250 mg, 5 eq), and triethylamine (44 µL, 1.1 eq) were combined in dichloromethane (5 mL). Sodium triacetoxyborohydride (270 mg, 4.5 eq) was added as a solid, and the mixture was stirred at room temperature for 48 h. A saturated aqueous solution of sodium carbonate was added, and the organic phase was separated. The aqueous phase was extracted twice with dichloromethane, dried over sodium sulfate, filtered, and concentrated under reduced pressure. The remaining oil was dissolved in ethyl acetate and added to a silica plug. The silica plug was eluted with ethyl acetate until the eluent was colorless, then the product was eluted with methanol, dried over sodium sulfate, and concentrated under reduced pressure to yield a yellow oil (48 mg, 34% yield).

^{1}H NMR ($CDCl_3$, 400 MHz): δ (ppm) = 8.71 (d, *J* = 5.1 Hz, 3H), 7.72 (d, *J* = 1.8 Hz, 3H), 7.36 (dd, *J* = 5.1, 1.7 Hz, 3H), 4.07 (s, 6H).

^{13}C{^{1}H} NMR ($CDCl_3$, 101 MHz): δ (ppm) = 160.55 (s), 150.19 (s), 138.85 (q, *J* = 34.1 Hz), 122.74 (q, *J* = 273.3 Hz), 118.82 (q, *J* = 3.6 Hz), 117.87 (q, *J* = 3.8 Hz), 60.55 (s).

^{19}F{^{1}H} NMR ($CDCl_3$, 376 MHz): δ (ppm) = −65.1 (s).

MS (ESI, UHPLC-MS (CH_3CO_2H), *m/z*): calculated for $C_{21}H_{15}F_9N_4$ + H, $[M+H]^+$: 495.1, found: 495.1.

General note about the synthesis of iron compounds: For the preparation of the following iron complexes, only the crystalline yield for the first crop of crystals is reported. Higher yields can be obtained if the supernatant is concentrated and recrystallized.

$[(TPA^{NMe2})Fe(MeCN)_2]OTf_2$

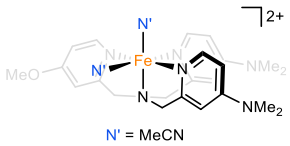

White solids TPA^{NMe2} (tris(4-(dimethylamino)-2-picolyl)amine) (30 mg, 1 eq) and $FeOTf_2 \cdot 2$ MeCN (31 mg, 1 eq) were each dissolved in 0.4 mL acetonitrile. The solution of $FeOTf_2$ was added to the solution of TPA^{NMe2}, instantly producing a pale orange-brown solution. The solution was filtered through Celite, and diethyl ether (2 mL) was layered on top of the filtrate. This mixture was placed in a freezer (−30 °C) until a purple-gray (this compound changes color with varying temperature) precipitate appeared. The precipitate was isolated by decanting the supernatant and drying under vacuum (50.7 mg, 83% yield).

^{1}H NMR (25 °C, CD_3CN, 400.15 MHz): δ (ppm) = 94.92 (s), 93.33 (s), 43.73 (s), 35.32 (s), 15.88 (s).

$^{19}F\{^{1}H\}$ NMR (25 °C, CD_3CN, 376 MHz): δ (ppm) = −77.1.

UV-vis (MeCN): nm [$cm^{-1}M^{-1}$]): 225 [20000], 283 [40000], 342 [3900].

MS (ESI, direct injection in MeCN, *m/z*): calculated for $C_{25}H_{33}N_7O_3F_3SFe$, $[M]^+$: 624.2, found: 624.3.

Electrochemistry: $E_{1/2}$ = 0.21 V vs Fc/Fc^+ (MeCN, 0.1 M $TBAPF_6$, BDD disk electrode).

[(TPA^{OMe})Fe(MeCN)$_2$]OTf$_2$

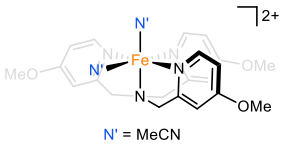

White solids TPA^{OMe} (tris(4-methoxy-2-picolyl)amine) (25 mg, 1 eq) and $FeOTf_2 \cdot 2$ MeCN (29 mg, 1 eq) were each dissolved in 0.25 mL acetonitrile. The solution of $FeOTf_2$ was added to the solution of TPA^{OMe}, instantly producing a purple-red solution. The solution was filtered through Celite, and diethyl ether (2 mL) was layered on top of the filtrate. This mixture was placed in a freezer (−30 °C) until dark purple needle-shaped crystals appeared. The precipitate was isolated by decanting the supernatant and drying under vacuum (34.7 mg, 64% yield).

^{1}H NMR (25 °C, CD_3CN, 400.15 MHz): δ (ppm) = 38.51 (s), 30.31 (s), 22.62 (s), 20.02 (s), 4.63 (s).

$^{19}F\{^1H\}$ NMR (25 °C, CD_3CN, 376 MHz): δ (ppm) = −78.1.

UV-vis (MeCN): nm [$cm^{-1}M^{-1}$]): 235 [24000], 339 [5100], 375 [4700].

MS (ESI, direct injection in MeCN, *m/z*): calculated for $C_{22}H_{24}N_4O_6F_3SFe$, $[M]^+$: 585.1, found: 585.2.

Electrochemistry: $E_{1/2}$ = 0.55 V vs Fc/Fc^+ (MeCN, 0.1 M $TBAPF_6$, BDD disk electrode).

[(TPA^{CF3})Fe(MeCN)$_2$]OTf$_2$

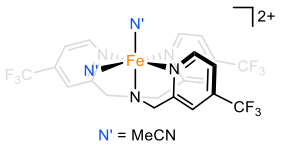

Yellow oil TPA^{CF3} (tris(4-(trifluoromethyl)-2-picolyl)amine) (72 mg, 1 eq) and white solid $FeOTf_2 \cdot 2$ MeCN (63 mg, 1 eq) were each dissolved in 0.5 mL acetonitrile. The solution of $FeOTf_2$ was added to the solution of TPA^{CF3}, instantly producing a purple-red solution. The solution was filtered through Celite, and diethyl ether (2 mL) was layered on top of the filtrate. This mixture was placed in a freezer (−30 °C) until dark red-brown crystals appeared. The precipitate was isolated by decanting the supernatant and drying under vacuum (47.5 mg, 35% yield).

^{1}H NMR (25 °C, CD_3CN, 400.15 MHz): δ (ppm) = 11.07 (s), 8.43 (s), 5.86 (s), 3.66 (s).

$^{19}F\{^1H\}$ NMR (25 °C, CD_3CN, 376 MHz): δ (ppm) = −65.9 (s), −78.9 (s).

UV-vis (MeCN): nm [$cm^{-1}M^{-1}$]): 225 [9900], 262 [13000], 388 [6600], 428 [8900].

MS (ESI, direct injection in MeCN, *m/z*): calculated for $C_{22}H_{15}N_4O_3F_{12}SFe$, $[M]^+$: 699.0, found: 699.0.

Electrochemistry: $E_{p/2}$ = 1.09 V (irreversible) vs Fc/Fc^+ (MeCN, 0.1 M $TBAPF_6$, BDD disk electrode).

BPM – dipyridyl substitution

2,2'-(ethene-1,1-diyl)bis(4-(dimethylamino)pyridine)

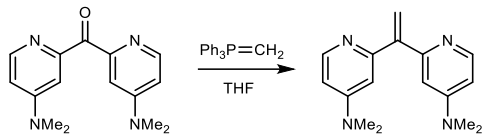

Note: This compound was prepared with modifications to the literature procedure for 2,2'-(ethene-1,1-diyl)dipyridine.[13] Notably, poor performance was observed when methylenetriphenylphosphorane was generated *in situ*, presumably due to residual potassium salts (i.e., KBr).

Bis(4-dimethylaminopyridin-2-yl)methanone (406 mg, 1.5 mmol, 1 eq) was suspended in anhydrous tetrahydrofuran (15 mL, 0.1 M) in a glovebox and cooled to −30 °C, after which isolated methylenetriphenylphosphorane (435 mg, 1.58 mmol, 1.05 eq) was added in one portion. This mixture was warmed to room temperature and allowed to react for at least 4 h (reaction times up to overnight have no deleterious impact). Outside of the glovebox, the reaction was quenched with minimal water and concentrated to yield a viscous orange-red oil. The oil was purified by silica gel column chromatography by loading with dichloromethane, eluting the triphenylphosphine oxide with 3:1 ethyl acetate:acetone plus 1% triethylamine, then eluting the product with acetone plus 1% triethylamine to afford a white crystalline solid (346 mg, 86% yield).

R_f = 0.3 (acetone plus 1% triethylamine; TLC plates treated with triethylamine).

^{1}H NMR ($CDCl_3$, 400 MHz): δ (ppm) = 8.29 (d, *J* = 5.9 Hz, 2H), 6.67 (d, *J* = 2.7 Hz, 2H), 6.46 (dd, *J* = 5.9, 2.6 Hz, 2H), 5.94 (s, 2H), 3.00 (s, 12H).

^{13}C{^{1}H} NMR ($CDCl_3$, 101 MHz): δ (ppm) = 158.66 (s), 154.77 (s), 150.57 (s), 149.32 (s), 118.66 (s), 106.38 (s), 105.47 (s), 39.18 (s).

HRMS (ESI, TOF (CH_3CO_2H), *m/z*): calculated for $C_{16}H_{20}N_4$ + H, $[M+H]^+$: 269.1761, found: 269.1763.

2,2'-(ethane-1,1-diyl)bis(4-(dimethylamino)pyridine)

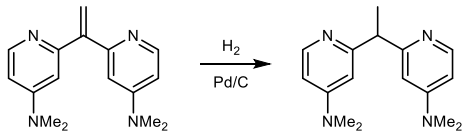

2,2'-(ethene-1,1-diyl)bis(4-(dimethylamino)pyridine) (268 mg, 1 mmol, 1 eq), Pd/C (43 mg, 5% by mass Pd, 0.02 eq), and activated carbon (134 mg, 0.5 mass eq) were suspended in methanol (10 mL, 0.1 M). The headspace of this mixture was purged with nitrogen and then hydrogen. A hydrogen atmosphere was maintained using a balloon, and the mixture was allowed to react for 12 h. The suspension was allowed to settle, and the solution was filtered through Celite. The remaining solids were washed with methanol, and the supernatant was filtered through Celite. The combined solution was concentrated, dissolved in dichloromethane, dried over sodium sulfate, and concentrated again to afford an off-white

crystalline solid after gentle heating under vacuum. (247 mg, 91% yield). This material was used without further purification.

^{1}H NMR ($CDCl_3$, 400 MHz): δ (ppm) = 8.19 (d, *J* = 6.0 Hz, 2H), 6.58 (d, *J* = 2.6 Hz, 2H), 6.34 (dd, *J* = 6.0, 2.6 Hz, 2H), 4.21 (q, *J* = 7.2 Hz, 1H), 2.95 (s, 12H), 1.71 (d, *J* = 7.2 Hz, 3H).

^{13}C{^{1}H} NMR ($CDCl_3$, 101 MHz): δ (ppm) = 164.30 (s), 154.84 (s), 149.03 (s), 105.02 (s), 104.81 (s), 50.39 (s), 39.13 (s), 19.94 (s).

MS (ESI, UHPLC-MS (CH_3CO_2H), *m/z*): calculated for $C_{16}H_{22}N_4$ + H, $[M+H]^+$: 271.2, found: 271.2.

HRMS (ESI, TOF (CH_3CO_2H), *m/z*): calculated for $C_{16}H_{22}N_4$ + H, $[M+H]^+$: 271.1917, found: 271.1919.

BPM^{NMe2} (6-(1,1-bis(4-(dimethylamino)pyridin-2-yl)ethyl)-2,2'-bipyridine)

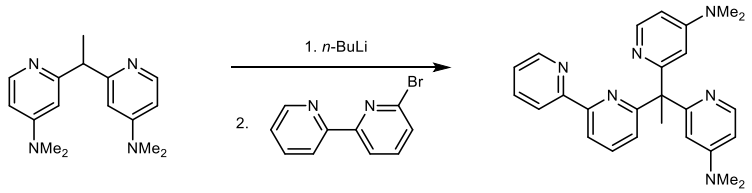

This compound was prepared by analogy to the parent ligand.[3] In a Schlenk tube under nitrogen, 2,2'-(ethane-1,1-diyl)bis(4-(dimethylamino)pyridine (135 mg, 0.5 mmol, 1 eq) was

dissolved in 2 mL dry tetrahydrofuran and cooled in a dry ice/acetone bath. A 1.6 M *n*-BuLi solution in hexanes (0.31 mL, 0.5 mmol, 1 eq) was added dropwise via syringe, and the solution turned yellow-orange. The mixture was stirred for 45 additional minutes, then 6-bromo-2,2'-bipyridine (118 mg, 0.5 mmol, 1 eq) was added as a solution in 0.5 mL tetrahydrofuran. The solution was warmed to room temperature and stirred for 16 h, after which time the reaction was quenched with water. The solution was concentrated, transferred to a separatory funnel, and extracted with dichloromethane. The combined organic fractions were concentrated and purified via column chromatography on neutral alumina using methanol:dichloromethane (1:49) to afford a waxy colorless solid. (163 mg, 77% yield).

R_f = 0.2 (methanol; TLC plates treated with methanol).

^{1}H NMR ($CDCl_3$, 400 MHz): δ (ppm) = 8.56 (ddd, *J* = 4.8, 1.9, 0.9 Hz, 1H), 8.31 (dt, *J* = 8.1, 1.1 Hz, 1H), 8.19 (dd, *J* = 5.8, 0.6 Hz, 2H), 8.15 (dd, *J* = 7.8, 0.9 Hz, 1H), 7.65 (td, *J* = 7.7, 1.8 Hz, 1H), 7.60 (t, *J* = 7.8 Hz, 1H), 7.17 (ddd, *J* = 7.5, 4.8, 1.3 Hz, 1H), 7.11 (dd, *J* = 7.9, 0.9 Hz, 1H), 6.31 – 6.25 (m, 4H), 2.79 (s, 12H), 2.33 (s, 3H).

$^{13}C\{^1H\}$ NMR ($CDCl_3$, 101 MHz): δ (ppm) = 166.41 (s), 165.44 (s), 156.89 (s), 154.50 (s), 154.27 (s), 148.86 (s), 148.79 (s), 136.66 (s), 136.48 (s), 124.42 (s), 123.30 (s), 121.47 (s), 117.99 (s), 106.72 (s), 104.38 (s), 60.37 (s), 39.04 (s), 27.16 (s).

MS (ESI, UHPLC-MS (CH_3CO_2H), *m/z*): calculated for $C_{26}H_{28}N_6$ + H, $[M+H]^+$: 425.3, found: 425.3.

HRMS (ESI, TOF (CH_3CO_2H), *m/z*): calculated for $C_{26}H_{28}N_6$ + H, $[M+H]^+$: 425.2448, found: 425.2448.

bis(4-methoxypyridin-2-yl)methanone

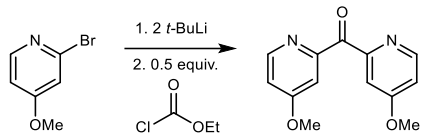

This compound was prepared by analogy to the known analogue, bis(4-(dimethylamino)pyridin-2-yl)methanone.[5] In a 100 mL flask under nitrogen, 2-bromo-4-methoxypyridine (0.7 g, 3.7 mmol, 1 eq) was dissolved in 30 mL dry diethyl ether and cooled in a dry ice/acetone bath. A 1.7 M *t*-BuLi solution in pentane (4.4 mL, 7.4 mmol, 2 eq) was added dropwise via syringe, and the solution slowly turned red-orange. The mixture was stirred for 5 additional minutes before neat ethyl chloroformate (0.18 mL, 1.8 mmol, 0.5 eq) was added all at once via syringe, after which the solution darkened. The solution was stirred 30 additional minutes in the dry ice/acetone bath, warmed to approximately 0 °C, and then quenched with water. The mixture was transferred to a separatory funnel and extracted with additional diethyl ether. The combined organic fractions were dried over sodium sulfate and concentrated under reduced pressure. The crude material was eluted through a plug of silica using acetone and then purified by silica gel column chromatography (3:1 ethyl acetate:acetone plus 1% triethylamine; R_f = 0.3) to yield an off-white solid (0.267 g, 59% yield). This material can be crystallized from cold 1:3 acetone:diethyl ether.

^{1}H NMR ($CDCl_3$, 400 MHz): δ (ppm) = 8.56 (dd, *J* = 5.7, 0.5 Hz, 2H), 7.61 (dd, *J* = 2.6, 0.5 Hz, 2H), 6.99 (dd, *J* = 5.7, 2.6 Hz, 2H), 3.93 (s, 6H).

^{13}C{^{1}H} NMR ($CDCl_3$, 101 MHz): δ (ppm) = 193.11 (s), 166.28 (s), 156.11 (s), 150.42 (s), 112.73 (s), 110.93 (s), 55.53 (s).

MS (ESI, UHPLC-MS (CH_3CO_2H), *m/z*): calculated for $C_{13}H_{12}N_2O_3$ + H, $[M+H]^+$: 245.1, found: 245.1.

HRMS (ESI, TOF (CH_3CO_2H), *m/z*): calculated for $C_{13}H_{12}N_2O_3$ + H, $[M+H]^+$: 245.0921, found: 245.0927.

2,2'-(ethene-1,1-diyl)bis(4-(methoxypyridine)

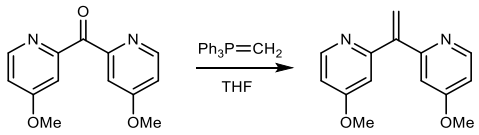

Note: This compound was prepared with modifications to the literature procedure for 2,2'-(ethene-1,1-diyl)dipyridine.[13] Notably, poor performance was observed when methylenetriphenylphosphorane was generated *in-situ*, presumably due to residual potassium salts (i.e., KBr).

Bis(4-methoxypyridin-2-yl)methanone (366 mg, 1.5 mmol, 1 eq) was dissolved in anhydrous tetrahydrofuran (15 mL, 0.1 M) in a glovebox and cooled to −30 °C, after which isolated methylenetriphenylphosphorane (435 mg, 1.58 mmol, 1.05 eq) was added in one portion.

This mixture was warmed to room temperature and allowed to react for at least 4 h (reaction times up to overnight have no deleterious impact). Outside of the glovebox, the reaction was quenched with minimal water and concentrated to yield a viscous orange-red oil. The oil was purified by silica gel column chromatography by loading with dichloromethane, eluting the triphenylphosphine oxide with 4:1 ethyl acetate:acetone plus 1% triethylamine, then eluting the product with 3:1 ethyl acetate:acetone plus 1% triethylamine to afford an off-white crystalline solid (269 mg, 74% yield).

R_f = 0.3 (4:1 ethyl acetate:acetone plus 1% triethylamine; TLC plates treated with triethylamine).

^{1}H NMR ($CDCl_3$, 400 MHz): δ (ppm) = 8.49 (d, *J* = 5.7 Hz, 2H), 6.95 (d, *J* = 2.4 Hz, 2H), 6.79 (dd, *J* = 5.7, 2.5 Hz, 2H), 6.04 (s, 2H), 3.86 (s, 6H).

^{13}C{^{1}H} NMR ($CDCl_3$, 101 MHz): δ (ppm) = 166.05 (s), 159.50 (s), 150.57 (s), 148.72 (s), 120.38 (s), 109.55 (s), 108.54 (s), 55.14 (s).

HRMS (ESI, TOF (CH_3CO_2H), *m/z*): calculated for $C_{14}H_{14}N_2O_2$ + H, $[M+H]^+$: 243.1128, found: 243.1133.

2,2'-(ethane-1,1-diyl)bis(4-methoxypyridine)

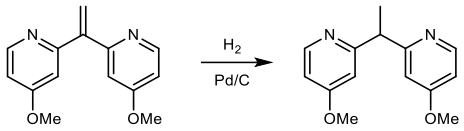

2,2'-(ethene-1,1-diyl)bis(4-methoxypyridine) (242 mg, 1 mmol, 1 eq), Pd/C (43 mg, 5% by mass Pd, 0.02 eq), and activated carbon (121 mg, 0.5 mass eq) were suspended in methanol (10 mL, 0.1 M). The headspace of this mixture was purged with nitrogen and then hydrogen. A hydrogen atmosphere was maintained using a balloon, and the mixture was allowed to react for 12 h. The suspension was allowed to settle, and the solution was filtered through Celite. The remaining solids were washed with methanol, and the supernatant was filtered through Celite. The combined solution was concentrated and purified by column chromatography to afford a white solid (127 mg, 52% yield).

Chromatography: Silica was slurry-packed with 1:19 methanol:dichloromethane then equilibrated with 1:49 methanol:dichloromethane. A gradient of 1:49 to 1:19 methanol:dichloromethane was used to elute the product, as well as a dimeric product characterized below.

R_f = 0.3 (1:19 methanol:dichloromethane).

^{1}H NMR ($CDCl_3$, 400 MHz): δ (ppm) = 8.36 (d, *J* = 5.8 Hz, 2H), 6.81 (d, *J* = 2.5 Hz, 2H), 6.64 (dd, *J* = 5.7, 2.5 Hz, 2H), 4.34 (q, *J* = 7.2 Hz, 1H), 3.79 (s, 6H), 1.71 (d, *J* = 7.2 Hz, 3H).

$^{13}C\{^{1}H\}$ NMR ($CDCl_3$, 101 MHz): δ (ppm) = 166.09 (s), 165.52 (s), 150.34 (s), 108.26 (s), 107.90 (s), 55.03 (s), 49.99 (s), 19.67 (s).

MS (ESI, UHPLC-MS (CH_3CO_2H), *m/z*): calculated for $C_{14}H_{16}N_2O_2$ + H, $[M+H]^+$: 245.1, found: 245.1.

HRMS (ESI, TOF (CH_3CO_2H), *m/z*): calculated for $C_{14}H_{16}N_2O_2$ + H, $[M+H]^+$: 245.1285, found: 245.1287.

Byproduct from synthesis of 2,2'-(ethane-1,1-diyl)bis(4-methoxypyridine):

2,2',2'',2'''- 2,2',2'',2'''-(butane-1,1,3,3-tetrayl)tetrakis(4-methoxypyridine)

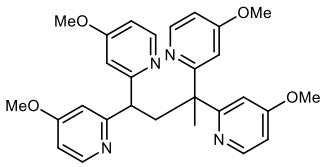

Isolated from the above reaction as a pale oil (75.6 mg, 31% yield).

R_f = 0.1 (1:19 methanol:dichloromethane).

^{1}H NMR ($CDCl_3$, 400 MHz): δ (ppm) = 8.31 (dd, *J* = 5.6, 0.9 Hz, 2H), 8.27 (dd, *J* = 5.7, 0.9 Hz, 2H), 6.78 (d, *J* = 2.5 Hz, 2H), 6.70 (d, *J* = 2.2 Hz, 2H), 6.55 (dd, *J* = 2.5, 1.1 Hz, 2H), 6.53 (dd, *J* = 2.4, 1.1 Hz, 2H), 4.27 (t, *J* = 6.0 Hz, 1H), 3.77 (s, 6H), 3.74 (s, 6H), 3.40 (d, *J* = 5.8 Hz, 2H), 1.72 (s, 3H).

$^{13}C\{^{1}H\}$ NMR ($CDCl_3$, 101 MHz): δ (ppm) = 168.19 (s), 165.72 (s), 165.58 (s), 165.11 (s), 149.76 (s), 149.64 (s), 108.52 (s), 108.12 (s), 107.20 (s), 54.96 (s), 54.87 (s), 52.99 (s), 51.92 (s), 44.21 (s), 25.63 (s).

HRMS (ESI, TOF (CH_3CO_2H), *m/z*): calculated for $C_{28}H_{30}N_4O_4$ + H, $[M+H]^+$: 487.2340, found: 487.2361.

BPM^{OMe} (6-(1,1-bis(4-methoxypyridin-2-yl)ethyl)-2,2'-bipyridine)

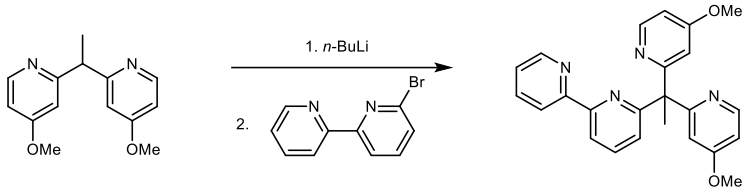

This compound was prepared by analogy to the parent ligand.[3] In a Schlenk tube under nitrogen, 2,2'-(ethane-1,1-diyl)bis(4-methoxypyridine (122 mg, 0.5 mmol, 1 eq) was dissolved in 2 mL dry tetrahydrofuran and cooled in a dry ice/acetone bath. A 1.6 M *n*-BuLi solution in hexanes (0.31 mL, 0.5 mmol, 1 eq) was added dropwise via syringe, and the solution turned yellow-orange. The mixture was stirred for 45 additional minutes, then 6-bromo-2,2'-bipyridine (118 mg, 0.5 mmol, 1 eq) was added as a solution in 0.5 mL tetrahydrofuran. The solution was warmed to room temperature and stirred for 24 h, after which time the reaction was quenched with water. The solution was concentrated, transferred to a separatory funnel, and extracted with dichloromethane. The combined organic fractions were concentrated and purified via column chromatography to afford a white solid (166 mg, 83% yield).

Chromatography: Silica was slurry-packed with 1:49 methanol:dichloromethane then equilibrated with 1:99 methanol:dichloromethane. A gradient of 1:99 to 1:19 methanol:dichloromethane was used to elute the product.

R_f = 0.3 (1:9 methanol:dichloromethane).

^{1}H NMR ($CDCl_3$, 400 MHz): δ (ppm) = 8.56 (ddd, *J* = 4.9, 1.9, 1.0 Hz, 1H), 8.38 (dd, *J* = 5.6, 0.8 Hz, 2H), 8.20 (ddt, *J* = 8.8, 7.7, 1.1 Hz, 2H), 7.64 (td, *J* = 7.8, 0.9 Hz, 2H), 7.19 – 7.15 (m, 1H), 7.09 (dd, *J* = 7.8, 1.0 Hz, 1H), 6.60 (ddd, *J* = 5.6, 2.4, 0.9 Hz, 2H), 6.56 (dd, *J* = 2.4, 0.8 Hz, 2H), 3.66 (d, *J* = 0.9 Hz, 6H), 2.32 (d, *J* = 1.0 Hz, 3H).

^{13}C{^{1}H} NMR ($CDCl_3$, 101 MHz): δ (ppm) = 167.66 (s), 165.72 (s), 164.37 (s), 156.55 (s), 154.55 (s), 150.12 (s), 148.88 (s), 136.87 (s), 136.71 (s), 123.94 (s), 123.46 (s), 121.30 (s), 118.37 (s), 110.37 (s), 106.96 (s), 60.23 (s), 54.96 (s), 27.10 (s).

MS (ESI, UHPLC-MS (CH_3CO_2H), *m/z*): calculated for $C_{24}H_{22}N_4O_2$ + H, $[M+H]^+$: 399.2, found: 399.1.

HRMS (ESI, TOF (CH_3CO_2H), *m/z*): calculated for $C_{24}H_{22}N_4O_2$ + H, $[M+H]^+$: 399.1816, found: 399.1821.

2,2'-(ethane-1,1-diyl)bis(4-(trifluoromethyl)pyridine)

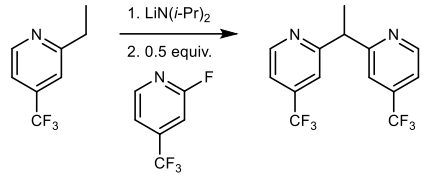

This compound was prepared by analogy to the procedure reported for the parent dipyridylethane.[14] In a Schlenk tube under nitrogen, 2-ethyl-4-(trifluoromethyl)pyridine (876 mg, 2 eq) was dissolved in THF (7 mL) and cooled to −78 °C while stirring. A 2.0 M solution of lithium diisopropylamide in THF/heptane/ethylbenzene (2.5 mL, 2 eq) was added dropwise via syringe, and the solution turned dark purple. The solution was warmed to room temperature for 5 minutes then cooled to −78 °C prior to dropwise addition of a cooled solution of 2-fluoro-4-(trifluoromethyl)pyridine (413 mg, 1 eq) in THF (3 mL). The reaction was warmed to room temperature after which it was stirred for 30 minutes then quenched with water. The mixture was concentrated, diluted in water, and extracted with dichloromethane. The organic extract was dried over sodium sulfate, concentrated, subjected to a silica plug with 1:4 ethyl acetate:hexane, and concentrated to a yellow oil that was used without further purification (0.15 g, 19% yield).

R_f = 0.3 (1:9 ethyl acetate:hexane).

^{1}H NMR ($CDCl_3$, 400 MHz): δ (ppm) = 8.73 (dt, *J* = 5.1, 0.8 Hz, 2H), 7.57 – 7.54 (m, 2H), 7.37 (ddd, *J* = 5.1, 1.7, 0.8 Hz, 2H), 4.61 (q, *J* = 7.2 Hz, 1H), 1.80 (d, *J* = 7.2 Hz, 3H).

$^{13}C\{^{1}H\}$ NMR ($CDCl_3$, 101 MHz): 164.46 (s), 150.34 (s), 138.89 (q, J = 33.9 Hz), 122.80 (q, J = 273.3 Hz), 118.10 (q, J = 3.6 Hz), 117.49 (q, J = 3.5 Hz), 49.90 (s), 19.79 (s).

$^{19}F\{^{1}H\}$ NMR ($CDCl_3$, 376 MHz): δ (ppm) = −64.8 (s).

MS (ESI, UHPLC-MS (CH_3CO_2H), *m/z*): calculated for $C_{14}H_{10}N_2F_6$ + H, $[M+H]^+$: 321.1, found: 321.1.

BPM^{CF3} (6-(1,1-bis(4-(trifluoromethyl)pyridin-2-yl)ethyl)-2,2'-bipyridine)

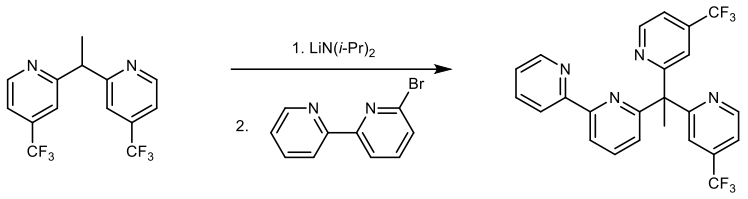

This compound was prepared by analogy to the parent ligand.[3] In a Schlenk tube under nitrogen, 2,2'-(ethane-1,1-diyl)bis(4-trifluoromethyl)pyridine (0.1 g, 1 eq) was dissolved in 3 mL tetrahydrofuran and cooled in a dry ice/acetone bath. A 2.0 M lithium diisopropylamide solution in THF/heptane/ethylbenzene (0.16 mL, 1.05 eq) was added dropwise via syringe, and the solution turned red. The mixture was stirred for 5 additional minutes then warmed to room temperature. The solution was returned to the dry ice/acetone bath before 6-bromo-2,2'-bipyridine (0.073 g, 1 eq) was added as a solid. The solution was warmed to room temperature then heated to 70 °C for 1.5 d, after which time the reaction was cooled to room temperature and quenched with water. The solution was concentrated, transferred to a separatory funnel, and extracted with dichloromethane. The combined organic fractions were dried over sodium sulfate, concentrated, and purified via silica gel column chromatography using 1:4 ethyl acetate:hexane to afford a viscous yellow oil (0.075 g, 51% yield).

R_f = 0.2 (1:4 ethyl acetate:hexane).

^{1}H NMR ($CDCl_3$, 400 MHz): δ (ppm) = 8.68 (dt, *J* = 5.1, 0.8 Hz, 2H), 8.57 (ddd, *J* = 4.8, 1.8, 0.9 Hz, 1H), 8.26 (dd, *J* = 7.9, 0.9 Hz, 1H), 7.98 (dt, *J* = 8.1, 1.1 Hz, 1H), 7.73 (t, *J* = 7.9

Hz, 1H), 7.62 (td, *J* = 7.7, 1.8 Hz, 1H), 7.41 (dt, *J* = 1.6, 0.8 Hz, 2H), 7.32 (ddd, *J* = 5.1, 1.7, 0.8 Hz, 2H), 7.23 – 7.15 (m, 2H), 2.33 (s, 3H).

$^{13}C\{^{1}H\}$ NMR ($CDCl_3$, 101 MHz): δ (ppm) = 167.10 (s), 162.96 (s), 155.88 (s), 154.91 (s), 149.53 (s), 148.97 (s), 138.11 (q, *J* = 33.7 Hz), 137.60 (s), 136.83 (s), 123.78 (s), 123.09 (s), 122.92 (q, *J* = 273.6 Hz), 121.08 (s), 119.57 (q, *J* = 3.8 Hz), 118.96 (s), 117.13 (q, *J* = 3.6 Hz), 60.54 (s), 27.10 (s).

$^{19}F\{^{1}H\}$ NMR ($CDCl_3$, 376 MHz): δ (ppm) = −64.7 (s).

MS (ESI, UHPLC-MS (CH_3CO_2H), *m/z*): calculated for $C_{24}H_{16}N_4F_6$ + H, $[M+H]^+$: 475.1, found: 475.1.

[(BPM^{NMe2})Fe(MeCN)$_2$]OTf$_2$

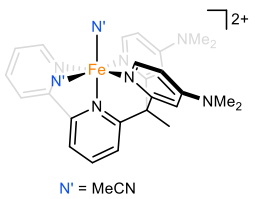

White solids BPM^{NMe2} (6-(1,1-bis(4-(dimethylamino)pyridin-2-yl)ethyl)-2,2'-bipyridine) (30 mg, 1 eq) and FeOTf$_2$ · 2 MeCN (31 mg, 1 eq) were each dissolved in 0.5 mL acetonitrile. The solution of FeOTf$_2$ was added to the solution of BPM^{NMe2}, instantly producing a purple solution. The solution was filtered through a glass microfilter, and diethyl ether (2 mL) was layered on top of the filtrate. This mixture was placed in a freezer (−30 °C) until a purple precipitate appeared. The precipitate was isolated by decanting the supernatant and drying under vacuum (50.7 mg, 83% yield).

^{1}H NMR (25 °C, CD$_3$CN, 400.15 MHz): δ (ppm) = 9.55 (d, *J* = 5.5 Hz, 1H), 8.49 (d, *J* = 6.8 Hz, 2H), 8.39 (d, *J* = 8.0 Hz, 1H), 8.27 (d, *J* = 7.9 Hz, 1H), 8.17 (td, *J* = 7.9, 0.9 Hz, 1H), 8.13 (t, *J* = 7.9 Hz, 1H), 7.94 (d, *J* = 8.0 Hz, 1H), 7.74 (t, *J* = 6.5 Hz, 1H), 7.04 (d, *J* = 2.7 Hz, 2H), 6.60 (dd, *J* = 6.9, 2.7 Hz, 2H), 3.07 (d, *J* = 1.0 Hz, 12H), 2.70 (s, 3H).

^{19}F{^{1}H} NMR (25 °C, CD$_3$CN, 376 MHz): δ (ppm) = −79.3.

UV-vis (MeCN): nm [cm^{-1}M^{-1}]): 331 [12000], 393 [4400], 498 [2800], 528 [3200].

MS (ESI, direct injection in MeCN, *m/z*): calculated for $C_{27}H_{28}N_6O_3F_3SFe$, $[M]^+$: 629.1, found: 629.2.

Electrochemistry: $E_{1/2}$ = 0.45 V vs Fc/Fc^+ (MeCN, 0.1 M $TBAPF_6$, BDD disk electrode).

[(BPM^{OMe})Fe(MeCN)$_2$]OTf$_2$

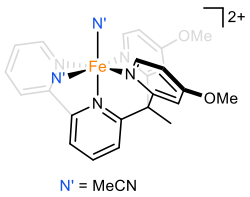

White solids BPM^{OMe} (6-(1,1-bis(4-methoxypyridin-2-yl)ethyl)-2,2'-bipyridine) (26 mg, 1 eq) and $FeOTf_2 \cdot 2$ MeCN (28.5 mg, 1 eq) were each dissolved in 0.3 mL acetonitrile. The solution of $FeOTf_2$ was added to the solution of BPM^{OMe}, instantly producing a purple solution. The solution was filtered through a glass microfilter, and diethyl ether (1.5 mL) was layered on top of the filtrate. This mixture was placed in a freezer (−30 °C) until a purple precipitate appeared. The precipitate was isolated by decanting the supernatant and drying under vacuum (50.2 mg, 92% yield).

^{1}H NMR (25 °C, CD_3CN, 400.15 MHz): δ (ppm) = 9.57 (d, *J* = 5.5 Hz, 1H), 8.94 (d, *J* = 6.5 Hz, 2H), 8.40 (d, *J* = 8.0 Hz, 1H), 8.28 (d, *J* = 7.9 Hz, 1H), 8.18 (dt, *J* = 13.5, 7.9 Hz, 2H), 7.99 (d, *J* = 7.9 Hz, 1H), 7.77 (t, *J* = 6.6 Hz, 1H), 7.46 (d, *J* = 2.6 Hz, 2H), 7.00 (dd, *J* = 6.7, 2.6 Hz, 2H), 3.93 (s, 6H), 2.74 (s, 3H).

^{19}F{^{1}H} NMR (25 °C, CD_3CN, 376 MHz): δ (ppm) = −79.3.

UV-vis (MeCN): nm [$cm^{-1}M^{-1}$]): 305 [24000], 338 [5500], 387 [3500], 496 [2900].

MS (ESI, direct injection in MeCN, *m/z*): calculated for $C_{25}H_{22}N_4O_5F_3SFe$, $[M]^+$: 603.1, found: 603.2.

Electrochemistry: $E_{1/2}$ = 0.69 V vs Fc/Fc^+ (MeCN, 0.1 M $TBAPF_6$, BDD disk electrode).

[(BPM^{CF3})Fe(MeCN)$_2$]OTf$_2$

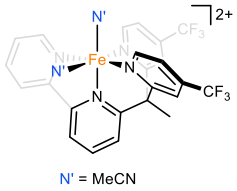

Yellow oil BPM^{CF3} (6-(1,1-bis(4-(trifluoromethyl)pyridin-2-yl)ethyl)-2,2'-bipyridine) (87.8 mg, 1 eq) and white solid $FeOTf_2 \cdot 2$ MeCN (80.6 mg, 1 eq) were each dissolved in 0.3 mL acetonitrile. The solution of $FeOTf_2$ was added to the solution of BPM^{CF3}, instantly producing an orange solution. The solution was filtered through a glass microfilter, and diethyl ether (1.5 mL) was layered on top of the filtrate. This mixture was placed in a freezer (−30 °C) until an orange-red precipitate appeared. The precipitate was isolated by decanting the supernatant and drying under vacuum (163.8 mg, 97% yield).

^{1}H NMR (25 °C, CD_3CN, 400.15 MHz): δ (ppm) = 9.57 (d, *J* = 5.6 Hz, 1H), 9.53 (d, *J* = 6.0 Hz, 2H), 8.42 (d, *J* = 7.9 Hz, 1H), 8.26 (dt, *J* = 15.7, 7.9 Hz, 3H), 8.15 (s, 2H), 8.04 (d, *J* = 7.8 Hz, 1H), 7.83 (t, *J* = 6.6 Hz, 1H), 7.68 (d, *J* = 5.9 Hz, 2H), 2.91 (s, 3H).

^{19}F{^{1}H} NMR (25 °C, CD_3CN, 376 MHz): δ (ppm) = −65.3, −79.3.

UV-vis (MeCN): nm [$cm^{-1}M^{-1}$]): 259 [16000], 301 [19000], 361 [4100], 425 [6000], 463 [5000].

MS (ESI, direct injection in MeCN, *m/z*): calculated for $C_{25}H_{16}N_4O_3F_9SFe$: 679.0, found: 679.2.

Electrochemistry: $E_{p/2}$ = 0.96 V (irreversible) vs Fc/Fc^+ (MeCN, 0.1 M $TBAPF_6$, BDD disk electrode).

D3. Additional voltammetry data related to *E*°

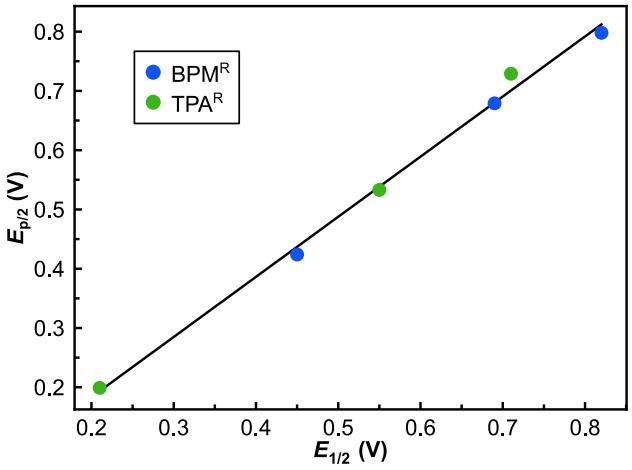

Figure D1. Correlation between half-wave ($E_{1/2}$) and half-peak ($E_{p/2}$) potentials for both $[(TPA^{R})Fe(MeCN)_2]^{2+}$ and $[(BPM^{R})Fe(MeCN)_2]^{2+}$ for R = NMe_2, OMe, H. Potentials are reported versus Fc/Fc^{+}.

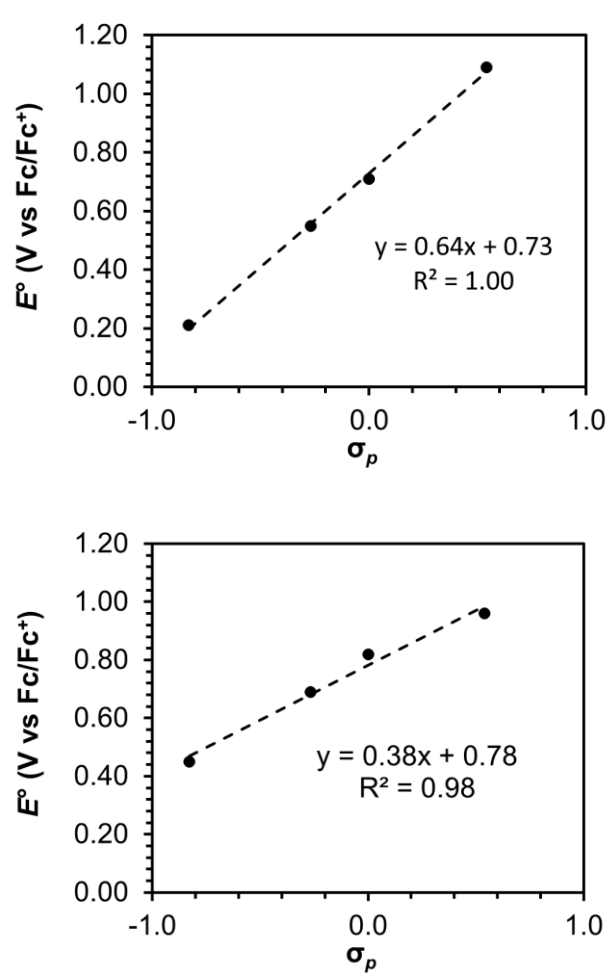

Figure D2. Electrochemical data for $[(TPA^{R})Fe(MeCN)_2]^{2+}$ (left) and $[(BPM^{R})Fe(MeCN)_2]^{2+}$ (right) analyzed using a Hammett parameter. $E°$ represents $E_{1/2}$ or $E_{p/2}$ and is plotted as a function of Hammett σ_p. From left to right, R = NMe_2, OMe, H, CF_3.

D4. Additional voltammetry data for R = CF_3

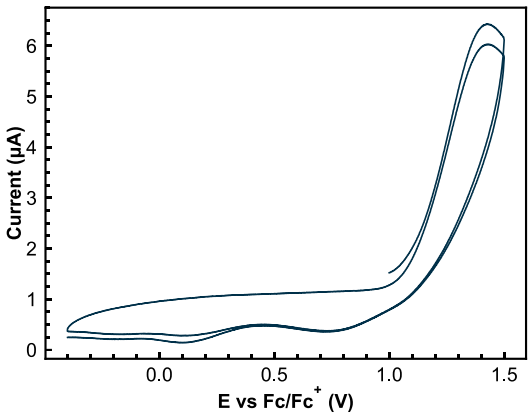

Figure D3. Cyclic voltammetry (2 scans at 100 mV/s) of $[(TPA^{CF3})Fe(MeCN)_2]^{2+}$ in acetonitrile using 0.1 M tetrabutylammonium hexafluorophosphate as supporting electrolyte.

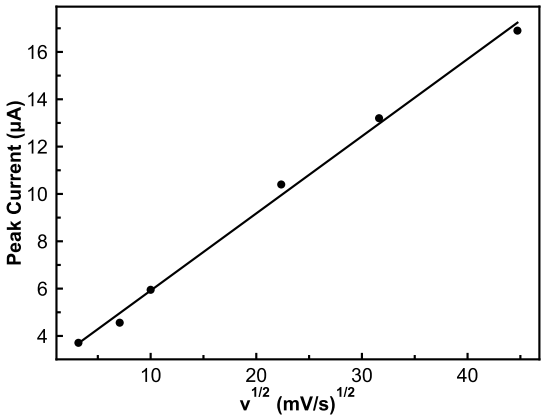

Figure D4. Randles–Ševčík plot from cyclic voltammograms of $[(TPA^{CF3})Fe(MeCN)_2]^{2+}$ in acetonitrile using 0.1 M tetrabutylammonium hexafluorophosphate as supporting electrolyte. The linear behavior is indicative of a freely diffusing, non-catalytic electroactive species, which, when combined with similar peak currents between scans, corroborates assignment of this redox feature as reversible.

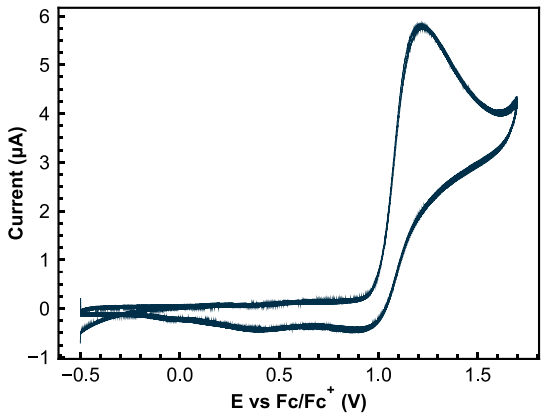

Figure D5. Cyclic voltammetry (2 scans at 100 mV/s) of $[(BPM^{CF3})Fe(MeCN)_2]^{2+}$ in acetonitrile using 0.1 M tetrabutylammonium hexafluorophosphate as supporting electrolyte.

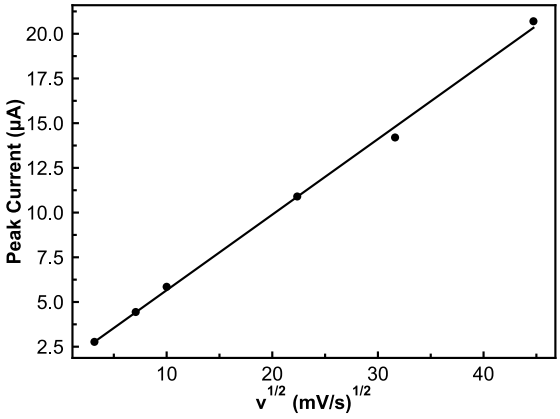

Figure D6. Randles–Ševčík plot from cyclic voltammograms of $[(BPM^{CF3})Fe(MeCN)_2]^{2+}$ in acetonitrile using 0.1 M tetrabutylammonium hexafluorophosphate as supporting electrolyte. The linear behavior is indicative of a freely diffusing, non-catalytic electroactive species, which, when combined with similar peak currents between scans, corroborates assignment of this redox feature as reversible.

D5. E_1 voltammetry

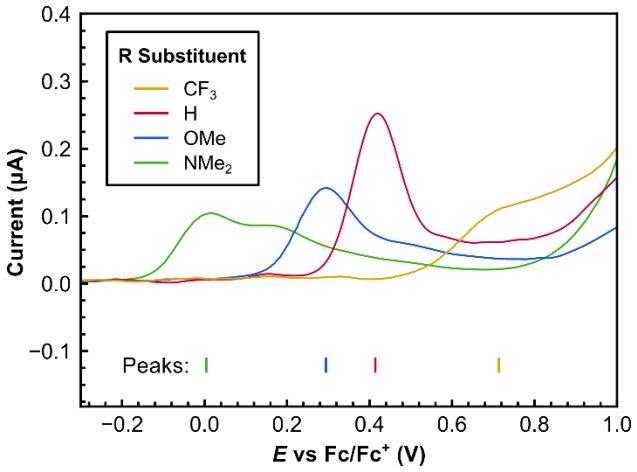

Figure D7. Differential pulse voltammetry of $[(TPA^{R})Fe(MeCN)_2]^{2+}$ in acetonitrile with 50 equiv. NH_3 using 0.05 M ammonium triflate as supporting electrolyte with BDD WE. Peak locations (indicated by vertical bars in plot) were picked using the peak picking function in EC-Lab.

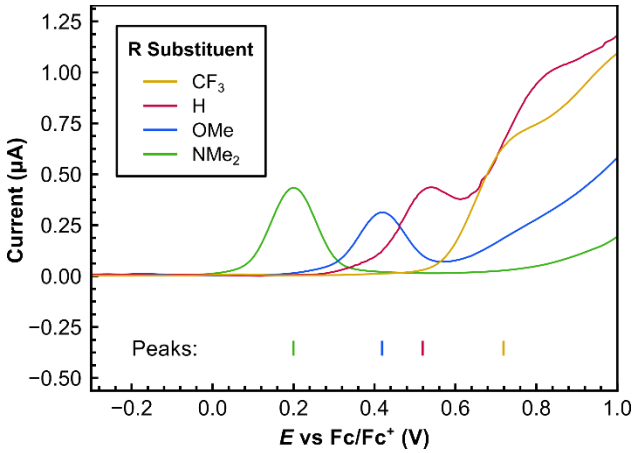

Figure D8. Differential pulse voltammetry of $[(BPM^{R})Fe(MeCN)_2]^{2+}$ in acetonitrile with 50 equiv. NH_3 using 0.05 M ammonium triflate as supporting electrolyte with BDD WE. Peak locations (indicated by vertical bars in plot) were picked using the peak picking function in EC-Lab.

D6. Catalytic controlled potential coulometry experiments

The data in the main text related to catalytic activity versus *E*° was obtained coulometrically. While such data is typically obtained from an assessment of catalytic current via voltammetric methods, the low faradaic efficiencies observed with some of the catalysts under our catalytic conditions make such analyses unadvisable. Lowered faradaic efficiencies are observed with more electron-donating R-substituents that also result in lower overall activity. This is partially due to the catalytic conditions required for uniform comparison of the systems, i.e., low overall ammonia concentration to prevent ligand demetallation for CF_3-substituted catalysts. Since the catalytic rate is dependent on ammonia concentration, using only 50 equiv. NH_3 results in lower rates and facilitates unproductive, reversible redox processes with early intermediates, for example $Fe^{II}–NH_3 \rightleftharpoons Fe^{III}–NH_2$, thus lowering the faradaic efficiency for N_2.

Coulometric analysis of turnover frequency can accurately reflect the intrinsic turnover frequency, provided that catalyst decomposition is negligible or equivalent between systems. Employing a high catalyst concentration (0.4 mM) as compared to the optimal concentration (0.05 mM) and a relatively short reaction time (8 h vs 48 h) both serve to mitigate effects related to catalyst loss.

Procedures for controlled potential coulometry (CPC)

Preparation of the BDD electrode: A 10 cm^2 boron-doped diamond (BDD) plate electrode (IKA) was physically attached to standard electrical wire, and the connection was covered

with Teflon tape. The surface area of the electrode submerged in solution was approximately 4 cm^2.

BDD has a surface that exists in various states of reduction (H-terminated) and oxidation (O-terminated).[15] In order to remove attached nitrogen and iron generated during controlled potential coulometry experiments and to ensure a reliable electrode surface prior to CPC measurements, the BDD plate electrode was oxidatively treated prior to use. First, the electrode was soaked in dilute nitric acid (~2 M) for 5 minutes. Then, a potential of 3.0 V vs Ag/AgCl was applied to the BDD electrode in a 0.5 M H_2SO_4 solution for 10 minutes. The electrode was then thoroughly rinsed with water prior to use.

Preparation of the platinum counter electrode: In order to ensure a highly active Pt surface for HER prior to CPC experiments, the Pt mesh counter electrode was soaked in concentrated hydrochloric acid for at least 5 minutes prior to usage.

Preparation of the custom Ag/AgOTf reference electrode: To ensure reliable potential measurements, the custom Ag/AgOTf reference electrode was prepared prior to each CPC experiment then a CV of ferrocene was measured. In a glass tube fitted with a Vycor porous glass frit attached by Teflon heatshrink tubing, an acetonitrile solution containing 5 mM AgOTf and 0.1 M $TBAPF_6$ or 0.05 M NH_4OTf was added. A silver wire was placed inside and the electrode was sealed.

Preparation of ammonia solutions: Saturated 2 M solutions[16] in acetonitrile were prepared by bubbling anhydrous ammonia through acetonitrile in a Schlenk tube under an

argon/ammonia atmosphere. More dilute stock solutions were immediately prepared from this saturated solution.

CPC: Inside an argon glovebox, a gas-tight electrochemical cell equipped with a 24/40 cap containing three tungsten rods for electrical contacts and a 14/20 joint carefully sealed with a Suba-Seal septum was prepared. A BDD plate electrode (A = 4 cm^2), high surface area platinum mesh electrode, and custom Ag/AgOTf reference electrode were connected to the 24/40 cap. All chemical reagents were then rapidly added to the cell to prevent evaporation of ammonia, then the cell was sealed with the 24/40 cap. Prior to each CPC experiment, a ZIR and CV were taken. No IR compensation was applied for CPC measurements. The CPC experiment was conducted for 8–48 h, then the cell was removed from the glovebox for analysis by gas chromatography. For headspace analysis, 100 μL of the headspace was injected into a GC-TCD for quantification using a lockable Hamilton syringe with a 26S gauge needle.

Table D1. Results of catalytic CPC experiments performed at 0.85 V vs Fc/Fc^+ for 8 h for examining the E_2 LFER with 0.4 mM [Fe] and 20 mM NH_3 (50 equivalents) in 10 mL acetonitrile total. Low ammonia concentrations were used to prevent demetallation.

Entry	Fe Source	Eq. N_2	Charge (C)	FE N_2 (%)	FE H_2 (%)
1	$[(TPA^{NMe2})Fe(MeCN)_2]OTf_2$	0.73	3.9	44	16
2	$[(TPA^{NMe2})Fe(MeCN)_2]OTf_2$	0.51	8.2	14	14
3	$[(TPA^{OMe})Fe(MeCN)_2]OTf_2$	1.5	24.8	14	16
4	$[(TPA^{OMe})Fe(MeCN)_2]OTf_2$	1.4	25	13	18
5	$[(TPA^{H})Fe(MeCN)_2]OTf_2$	3.3	18.3	42	44
6	$[(TPA^{H})Fe(MeCN)_2]OTf_2$	2.9	15.6	44	42
7	$[(TPA^{CF3})Fe(MeCN)_2]OTf_2$	4.0	14.4	65	56
8	$[(TPA^{CF3})Fe(MeCN)_2]OTf_2$	3.7	19.7	43	51
9	$[(BPM^{NMe2})Fe(MeCN)_2]OTf_2$	6.0	22.2	63	55
10	$[(BPM^{NMe2})Fe(MeCN)_2]OTf_2$	6.3	24.1	61	55
11	$[(BPM^{OMe})Fe(MeCN)_2]OTf_2$	12.8	34.4	87	75
12	$[(BPM^{OMe})Fe(MeCN)_2]OTf_2$	12.7	39.1	76	68
13	$[(BPM^{H})Fe(MeCN)_2]OTf_2$	14.4	41.0	82	73
14	$[(BPM^{H})Fe(MeCN)_2]OTf_2$	12.6	39.2	75	67
15	$[(BPM^{CF3})Fe(MeCN)_2]OTf_2$	7.4	18.5	94	82
16	$[(BPM^{CF3})Fe(MeCN)_2]OTf_2$	9.4	24.3	90	84

Table D2. Results of catalytic CPC experiments performed at 0.85 V vs Fc/Fc^+ for 48 h with 0.05 mM [Fe] and 100 mM NH_3 (2000 equivalents) in 10 mL acetonitrile total. Reload experiments are listed as x.1 and x.2 for the first and second experiment, respectively. The reload was stopped after 24 h when current ceased. LOQ indicates that too little gas was produced to exceed the limit of quantification.

Entry	Fe Source	Eq. N_2	Charge (C)	FE N_2 (%)	FE H_2 (%)
1	$[(BPM^{OMe})Fe(MeCN)_2]OTf_2$	383	108.9	102	83
1.1	$[(BPM^{OMe})Fe(MeCN)_2]OTf_2$	52	17.8	85	75
2	$[(BPM^{OMe})Fe(MeCN)_2]OTf_2$	381	113.9	98	86
3	$[(BPM^{OMe})Fe(MeCN)_2]OTf_2$	rinse test	113.7	rinse test	rinse test
3 – rinse test	$[(BPM^{OMe})Fe(MeCN)_2]OTf_2$	LOQ	1.5	LOQ	LOQ

Rinse test procedure: After performing 48 h of CPC (entry 3), the electrochemical cell was purged and opened inside of the glovebox to prevent exposure of the working electrode to ambient conditions. The working electrode was thoroughly rinsed with acetonitrile. Then, fresh acetonitrile containing 0.05 M NH_4OTf and 100 mM NH_3 (2000 equivalents) was added to the electrochemical cell, and the cell was resubjected to a potential of 0.85 V vs Fc/Fc^+ for 48 h (entry 3 – rinse test).

D7. CV of $[(BPM^{OMe})Fe(N')_2]^{2+}$ under catalytic conditions

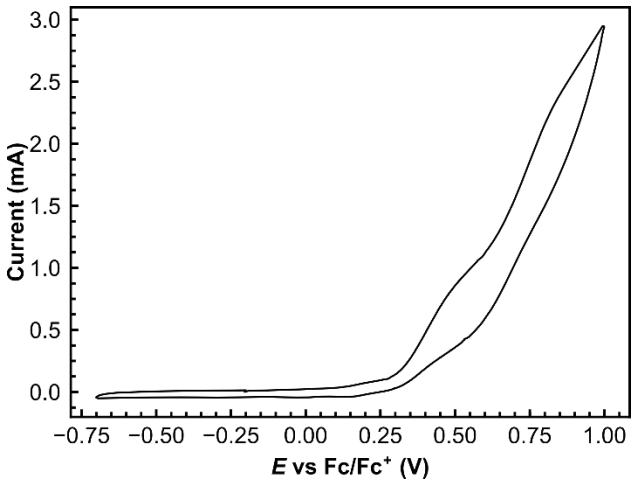

Figure D7. Cyclic voltammogram of 0.05 mM $[(BPM^{OMe})Fe(N')_2]^{2+}$ in acetonitrile containing 0.05 M ammonium triflate electrolyte and 2000 equiv. NH_3 (0.1 M). A BDD plate working electrode, platinum mesh counter electrode, and Ag/AgOTf reference electrode were used.

D8. NMR spectra of iron complexes used for Evans method

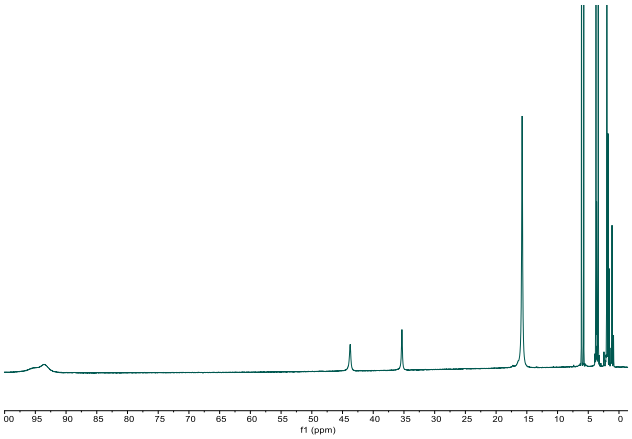

Figure D8. ^{1}H NMR spectrum of [(TPA^{NMe2})Fe(MeCN)$_2$]OTf$_2$ in CD_3CN at 25 °C.

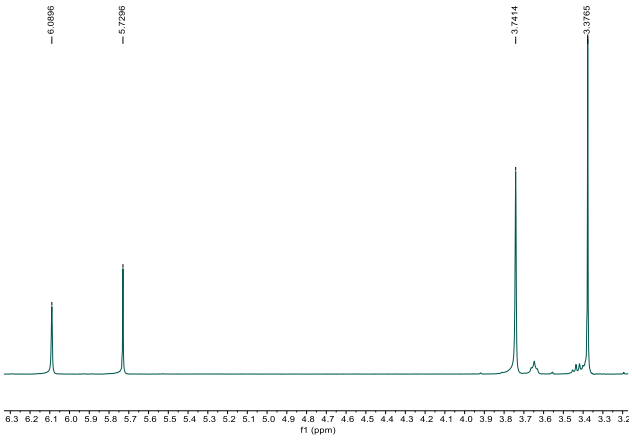

Figure D9. Trimethoxybenzene signals used for Evan's method for [(TPA^{NMe2})Fe(MeCN)$_2$]OTf$_2$ in CD_3CN at 25 °C. [Fe] = 0.011 M, Δf = 145 Hz, f = 400.15 MHz, μ_B = 4.4.

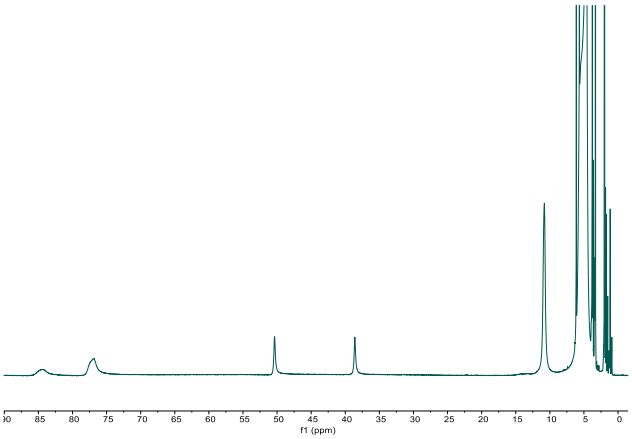

Figure D10. ^{1}H NMR spectrum of [(TPA^{NMe2})Fe(L)$_2$]OTf$_2$ (L = MeCN, NH$_3$), formed by mixing [(TPA^{NMe2})Fe(MeCN)$_2$]OTf$_2$ with 75 equivalents of NH$_3$ in CD$_3$CN at 25 °C.

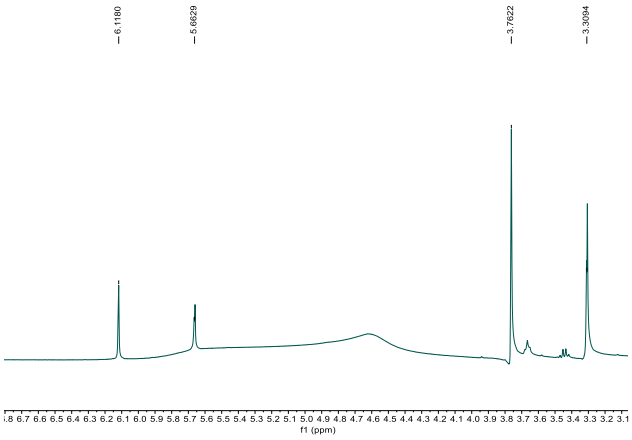

Figure D11. Trimethoxybenzene signals used for Evan's method for [(TPA^{NMe2})Fe(L)$_2$]OTf$_2$ (L = MeCN, NH$_3$), formed by mixing [(TPA^{NMe2})Fe(MeCN)$_2$]OTf$_2$ with 75 equivalents of NH$_3$ in CD$_3$CN at 25 °C. [Fe] = 0.011 M, Δf = 182 Hz, f = 400.15 MHz, μ_B = 4.9.

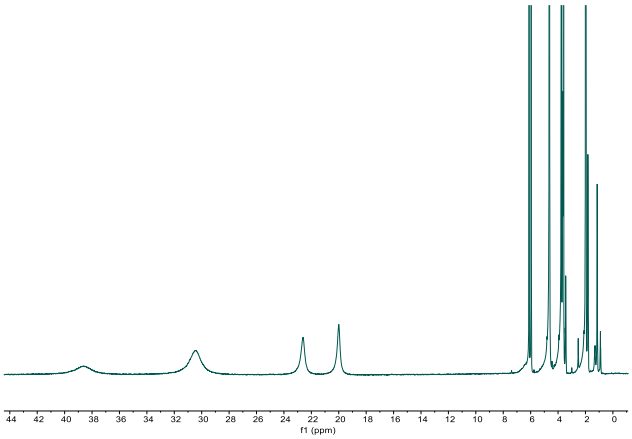

Figure D12. ^{1}H NMR spectrum of [(TPA^{OMe})Fe(MeCN)$_2$]OTf$_2$ in CD_3CN at 25 °C.

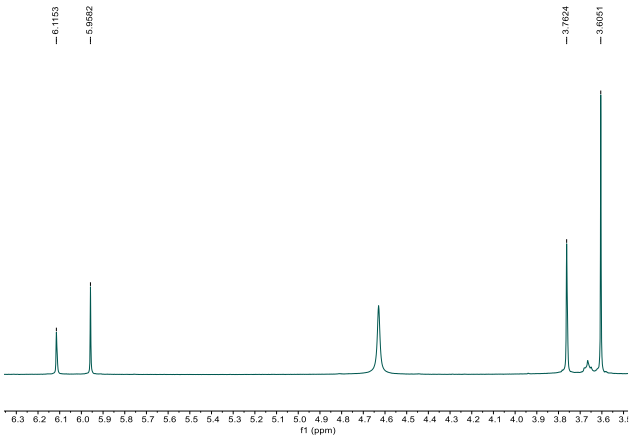

Figure D13. Trimethoxybenzene signals used for Evan's method for [(TPA^{OMe})Fe(MeCN)$_2$]OTf$_2$ in CD_3CN at 25 °C. [Fe] = 0.011 M, Δf = 62.9 Hz, f = 400.15 MHz, μ_B = 2.9.

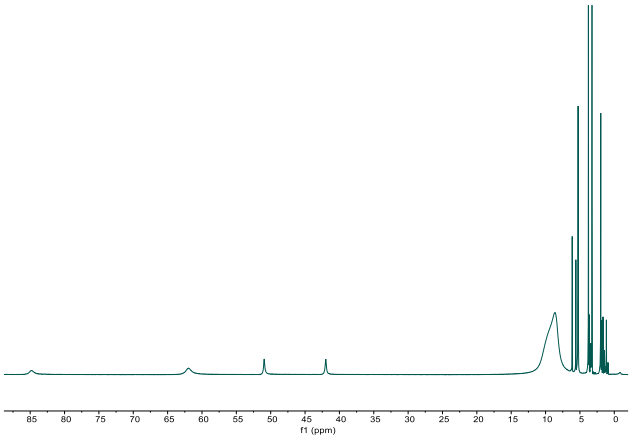

Figure D14. ^{1}H NMR spectrum of [(TPA^{OMe})Fe(L)$_2$]OTf$_2$ (L = MeCN, NH$_3$), formed by mixing [(TPA^{OMe})Fe(MeCN)$_2$]OTf$_2$ with 75 equivalents of NH$_3$ in CD$_3$CN at 25 °C.

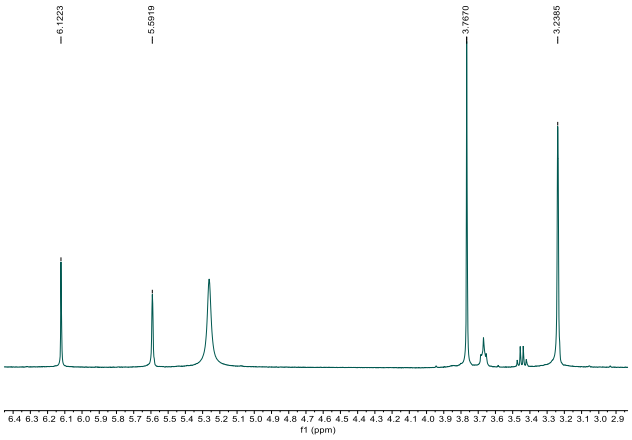

Figure D15. Trimethoxybenzene signals used for Evan's method for [(TPA^{OMe})Fe(L)$_2$]OTf$_2$ (L = MeCN, NH$_3$), formed by mixing [(TPA^{OMe})Fe(MeCN)$_2$]OTf$_2$ with 75 equivalents of NH$_3$ in CD$_3$CN at 25 °C. [Fe] = 0.011 M, $\Delta f = 212$ Hz, f = 400.15 MHz, $\mu_B = 5.4$.

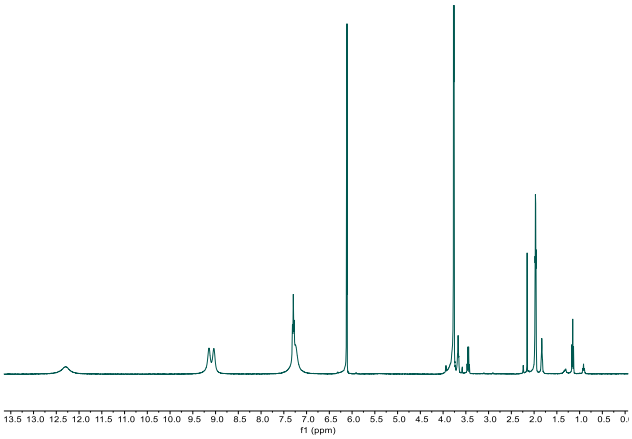

Figure D16. ^{1}H NMR spectrum of [(TPA)Fe(MeCN)$_2$]OTf$_2$ in CD_3CN at 25 °C.

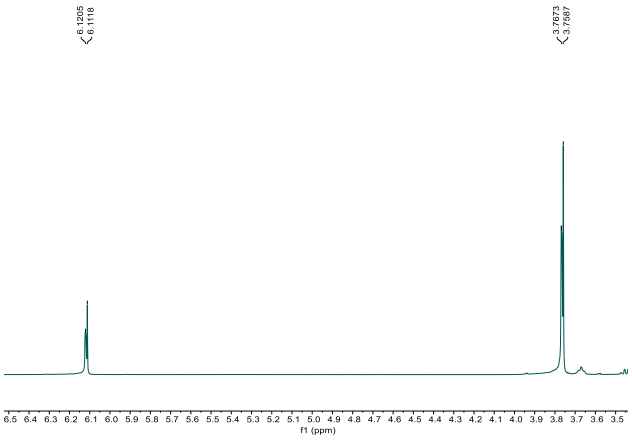

Figure D17. Trimethoxybenzene signals used for Evan's method for [(TPA)Fe(MeCN)$_2$]OTf$_2$ in CD_3CN at 25 °C. [Fe] = 0.011 M, $\Delta f = 3.46$ Hz, $f = 400.15$ MHz, $\mu_B = 0.68$.

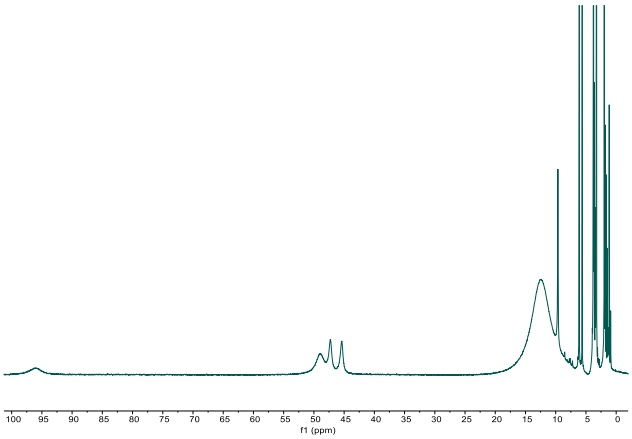

Figure D18. ^{1}H NMR spectrum of $[(TPA)Fe(L)_2]OTf_2$ (L = MeCN, NH_3), formed by mixing $[(TPA)Fe(MeCN)_2]OTf_2$ with 75 equivalents of NH_3 in CD_3CN at 25 °C.

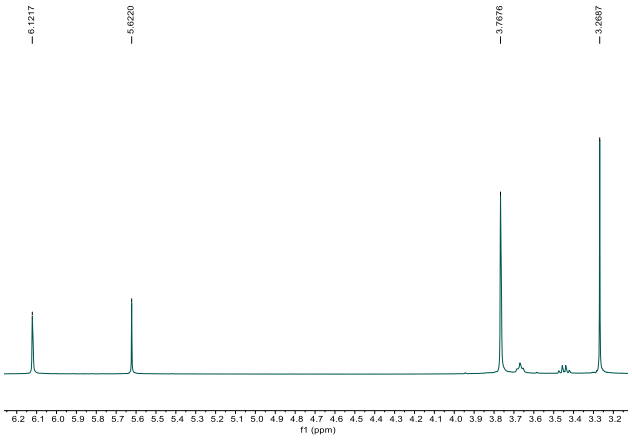

Figure D19. Trimethoxybenzene signals used for Evan's method for $[(TPA)Fe(L)_2]OTf_2$ (L = MeCN, NH_3), formed by mixing $[(TPA)Fe(MeCN)_2]OTf_2$ with 75 equivalents of NH_3 in CD_3CN at 25 °C. [Fe] = 0.011 M, Δf = 200 Hz, f = 400.15 MHz, μ_B = 5.2.

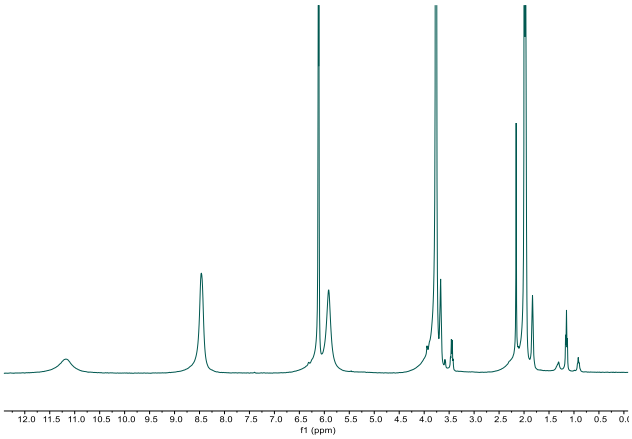

Figure D20. ^{1}H NMR spectrum of [(TPA^{CF3})Fe(MeCN)$_2$]OTf$_2$ in CD_3CN at 25 °C.

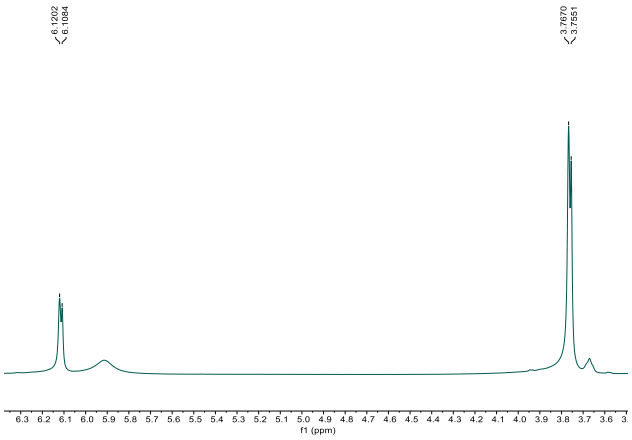

Figure D21. Trimethoxybenzene signals used for Evan's method for [(TPA^{CF3})Fe(MeCN)$_2$]OTf$_2$ in CD_3CN at 25 °C. [Fe] = 0.011 M, Δf = 4.74 Hz, f = 400.15 MHz, μ_B = 0.78.

Note: At the total NH_3/[Fe] concentrations required for NMR experiments, the TPA^{CF3} ligand dissociates, thus NMR data for [(TPA^{CF3})Fe(L)$_2$]OTf$_2$ is unavailable.

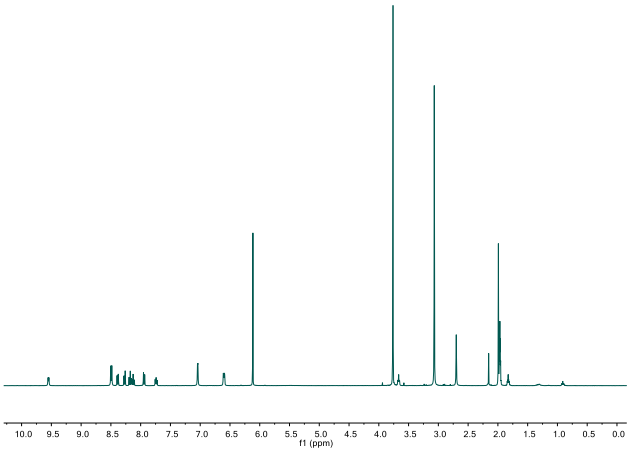

Figure D22. ^{1}H NMR spectrum of [(BPM^{NMe2})Fe(MeCN)$_2$]OTf$_2$ in CD_3CN at 25 °C.

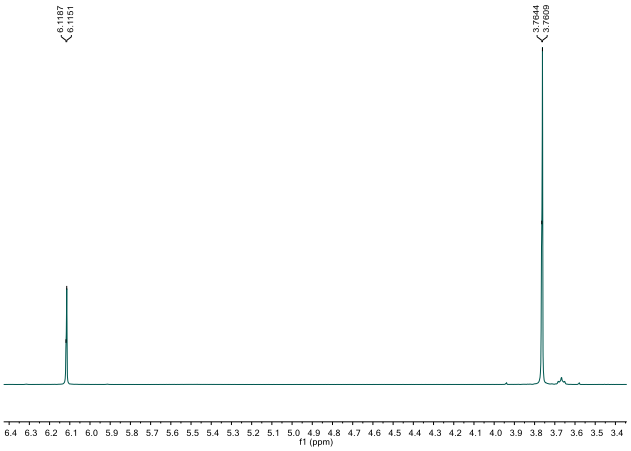

Figure D23. Trimethoxybenzene signals used for Evan's method for [(BPM^{NMe2})Fe(MeCN)$_2$]OTf$_2$ in CD_3CN at 25 °C. [Fe] = 0.011 M, $\Delta f = 1.4$ Hz, $f = 400.15$ MHz, $\mu_B = 0.43$.

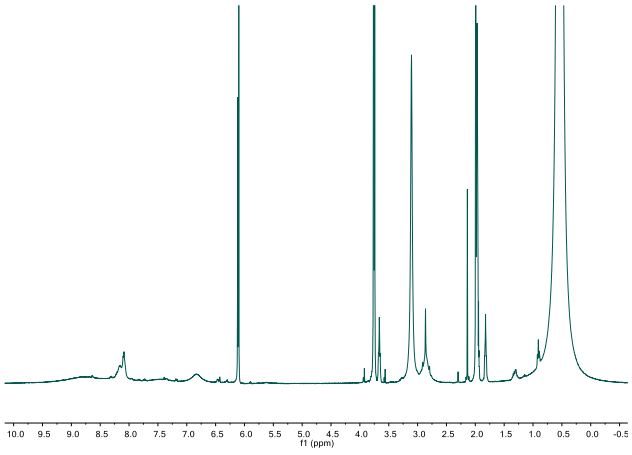

Figure D24. ^{1}H NMR spectrum of [(BPM^{NMe2})Fe(L)$_2$]OTf$_2$ (L = MeCN, NH$_3$), formed by mixing [(BPM^{NMe2})Fe(MeCN)$_2$]OTf$_2$ with 75 equivalents of NH$_3$ in CD$_3$CN at 25 °C.

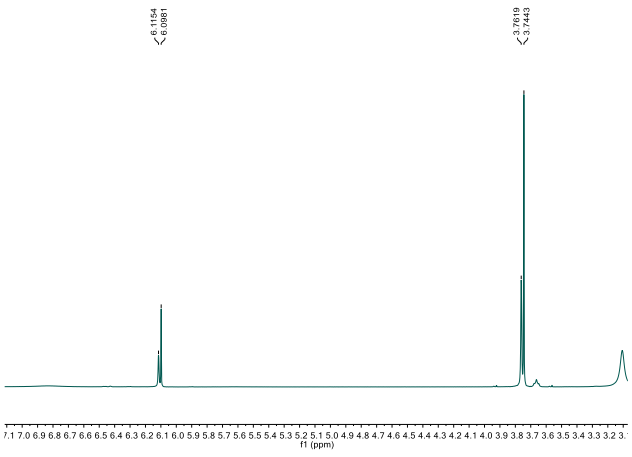

Figure D25. Trimethoxybenzene signals used for Evan's method for [(BPM^{NMe2})Fe(L)$_2$]OTf$_2$ (L = MeCN, NH$_3$), formed by mixing [(BPM^{NMe2})Fe(MeCN)$_2$]OTf$_2$ with 75 equivalents of NH$_3$ in CD$_3$CN at 25 °C. [Fe] = 0.011 M, $\Delta f = 7.0$ Hz, $f = 400.15$ MHz, $\mu_B = 0.96$.

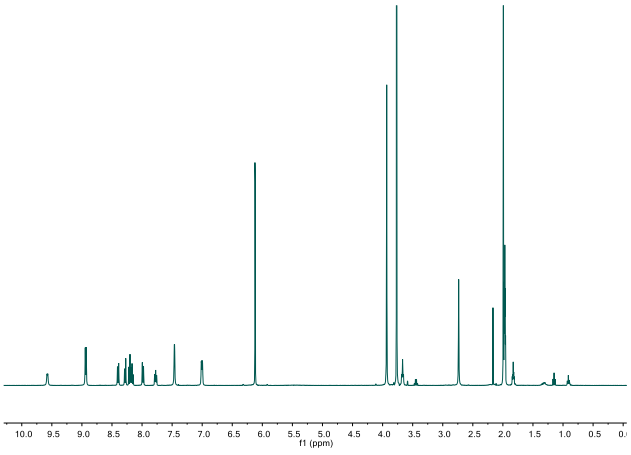

Figure D26. ^{1}H NMR spectrum of [(BPM^{OMe})Fe(MeCN)$_2$]OTf$_2$ in CD_3CN at 25 °C.

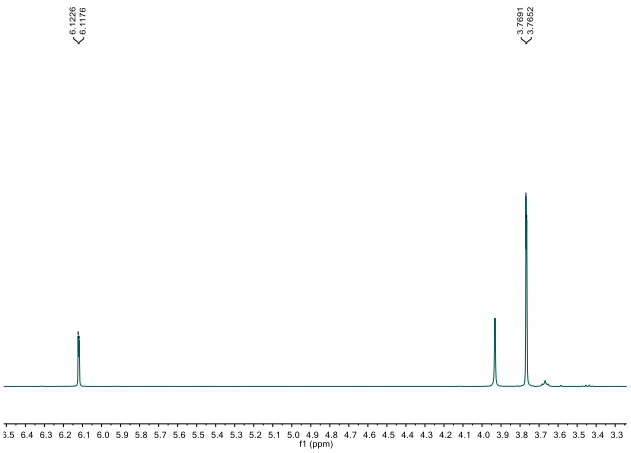

Figure D27. Trimethoxybenzene signals used for Evan's method for [(BPM^{OMe})Fe(MeCN)$_2$]OTf$_2$ in CD_3CN at 25 °C. [Fe] = 0.011 M, Δf = 1.8 Hz, f = 400.15 MHz, μ_B = 0.48.

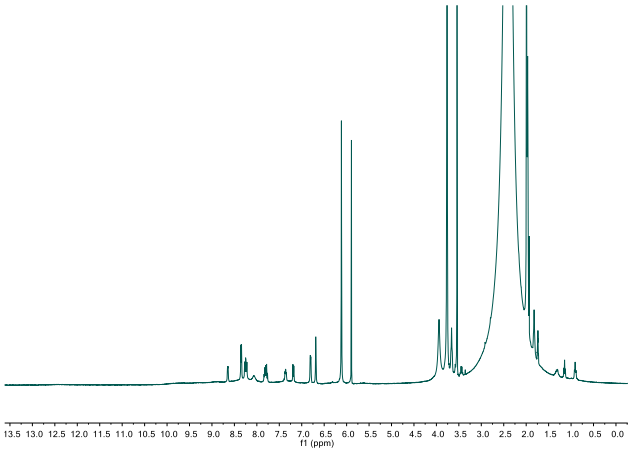

Figure D28. ^{1}H NMR spectrum of [(BPM^{OMe})Fe(L)$_2$]OTf$_2$ (L = MeCN, NH$_3$), formed by mixing [(BPM^{OMe})Fe(MeCN)$_2$]OTf$_2$ with 75 equivalents of NH$_3$ in CD$_3$CN at 25 °C.

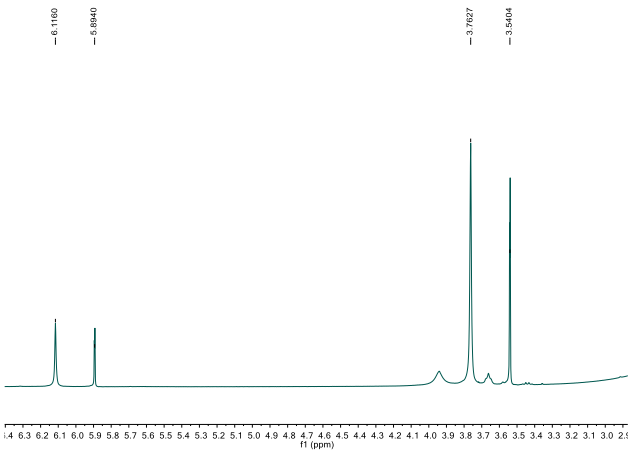

Figure D29. Trimethoxybenzene signals used for Evan's method for [(BPM^{OMe})Fe(L)$_2$]OTf$_2$ (L = MeCN, NH$_3$), formed by mixing [(BPM^{OMe})Fe(MeCN)$_2$]OTf$_2$ with 75 equivalents of NH$_3$ in CD$_3$CN at 25 °C. [Fe] = 0.011 M, Δf = 88.9 Hz, f = 400.15 MHz, μ_B = 3.4.

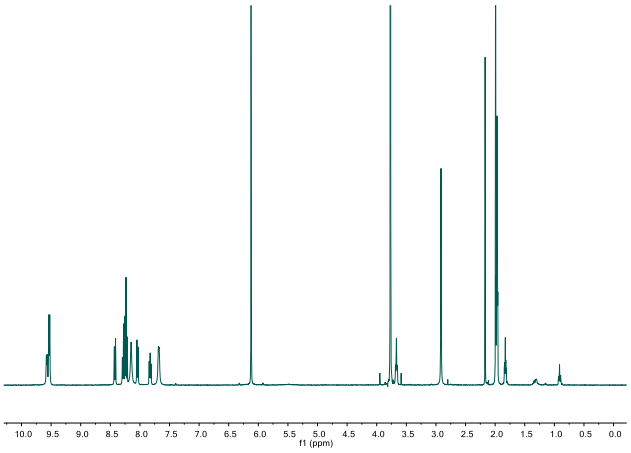

Figure D30. ^{1}H NMR spectrum of [(BPM^{CF3})Fe(MeCN)$_2$]OTf$_2$ in CD_3CN at 25 °C.

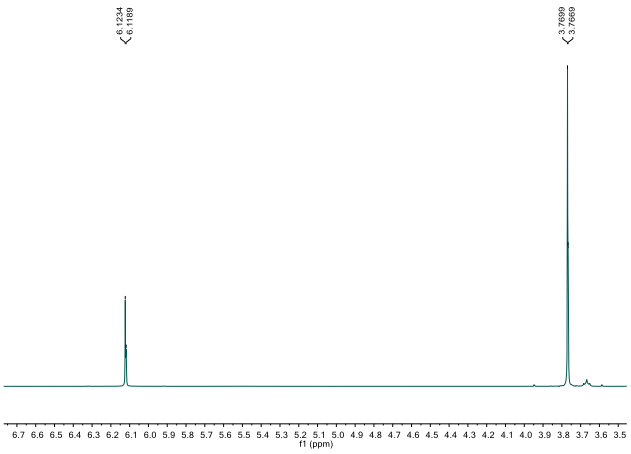

Figure D31. Trimethoxybenzene signals used for Evan's method for [(BPM^{CF3})Fe(MeCN)$_2$]OTf$_2$ in CD_3CN at 25 °C. [Fe] = 0.011 M, Δf = 1.5 Hz, f = 400.15 MHz, μ_B = 0.45.

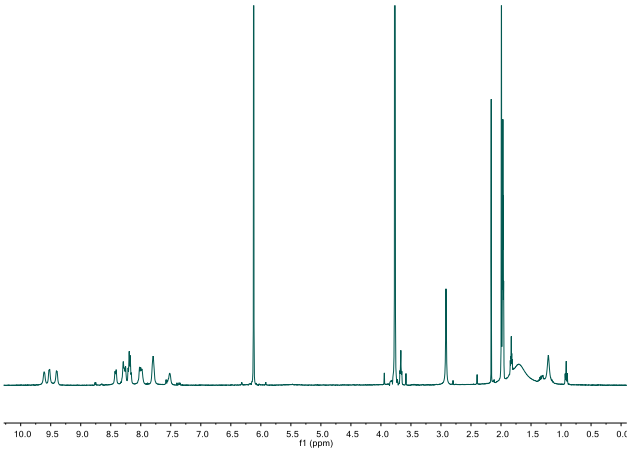

Figure D32. ^{1}H NMR spectrum of [(BPM^{CF3})Fe(L)$_2$]OTf$_2$ (L = MeCN, NH$_3$), formed by mixing [(BPM^{CF3})Fe(MeCN)$_2$]OTf$_2$ with 5 equivalents of NH$_3$ in CD$_3$CN at 25 °C. Demetallation occurs with 75 equivalents.

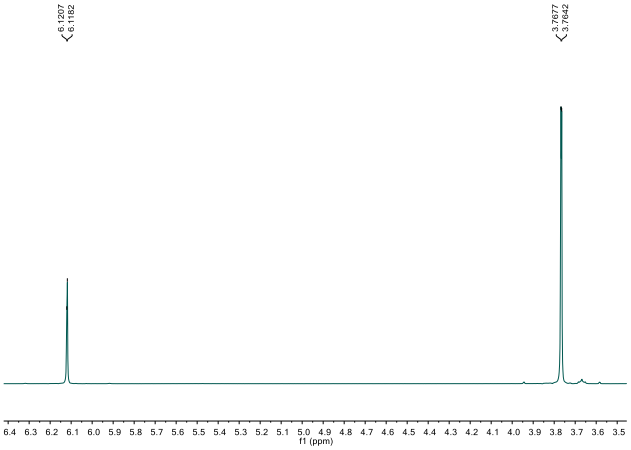

Figure D33. Trimethoxybenzene signals used for Evan's method for [(BPM^{CF3})Fe(L)$_2$]OTf$_2$ (L = MeCN, NH$_3$), formed by mixing [(BPM^{CF3})Fe(MeCN)$_2$]OTf$_2$ with 5 equivalents of NH$_3$ in CD$_3$CN at 25 °C. Demetallation occurs with 75 equivalents. [Fe] = 0.011 M, Δf = 1.2 Hz, f = 400.15 MHz, μ_B = 0.40.

D9. UV-vis titration data for stability against demetallation

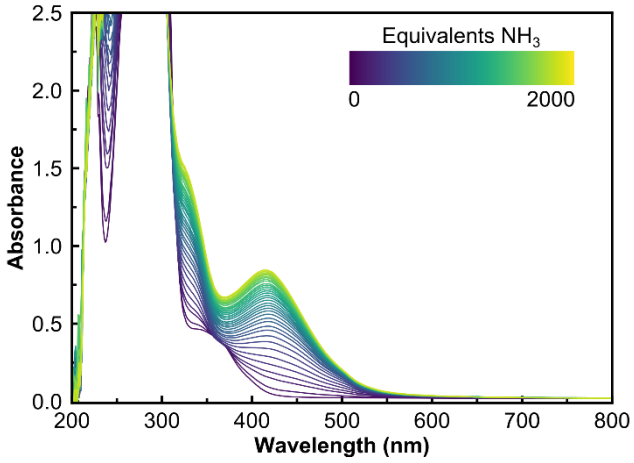

Figure D34. UV-vis spectra of acetonitrile solution containing 0.12 mM $[(TPA^{NMe2})Fe(MeCN)_2]OTf_2$ and varying equivalents NH_3 in a 1 cm cuvette.

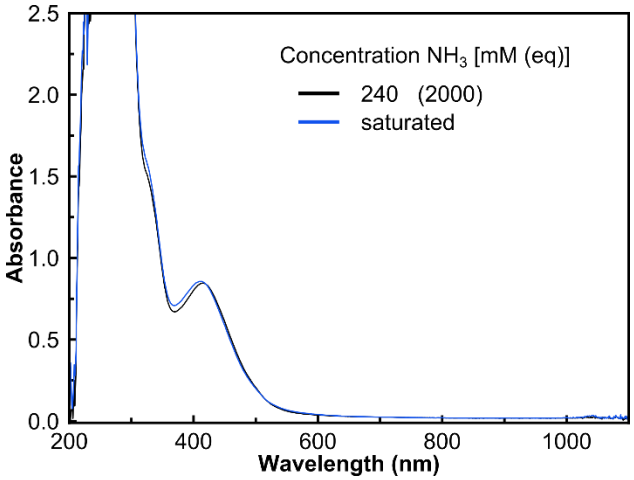

Figure D35. Selected UV-vis spectra used for determining the onset of demetallation for acetonitrile solution containing 0.12 mM $[(TPA^{NMe2})Fe(MeCN)_2]OTf_2$ and varying equivalents NH_3 in a 1 cm cuvette.

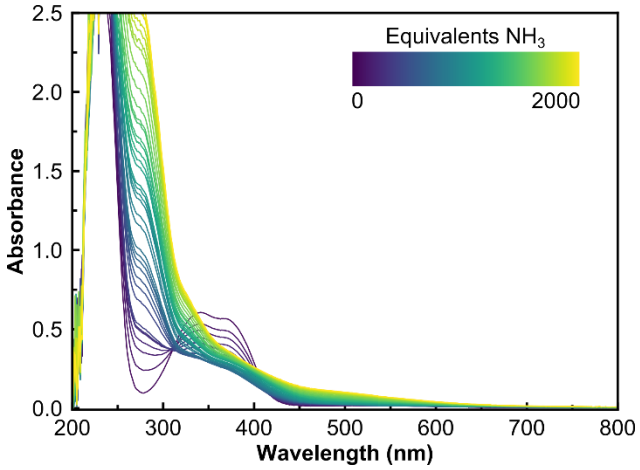

Figure D36. UV-vis spectra of acetonitrile solution containing 0.12 mM $[(TPA^{OMe})Fe(MeCN)_2]OTf_2$ and varying equivalents NH_3 in a 1 cm cuvette.

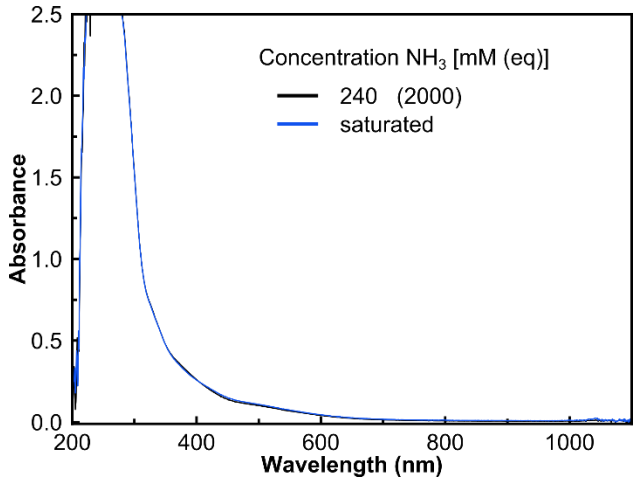

Figure D37. Selected UV-vis spectra used for determining the onset of demetallation for acetonitrile solution containing 0.12 mM $[(TPA^{OMe})Fe(MeCN)_2]OTf_2$ and varying equivalents NH_3 in a 1 cm cuvette.

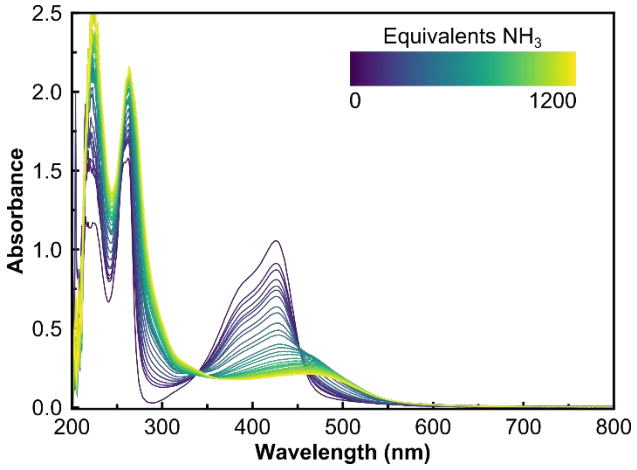

Figure D38. UV-vis spectra of acetonitrile solution containing 0.12 mM $[(TPA^{CF3})Fe(MeCN)_2]OTf_2$ and varying equivalents NH_3 in a 1 cm cuvette.

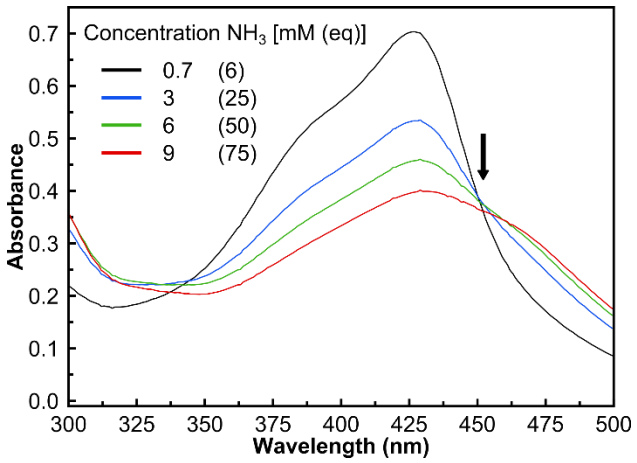

Figure D39. Selected UV-vis spectra used for determining the onset of demetallation for acetonitrile solution containing 0.12 mM $[(TPA^{CF3})Fe(MeCN)_2]OTf_2$ and varying equivalents NH_3 in a 1 cm cuvette.

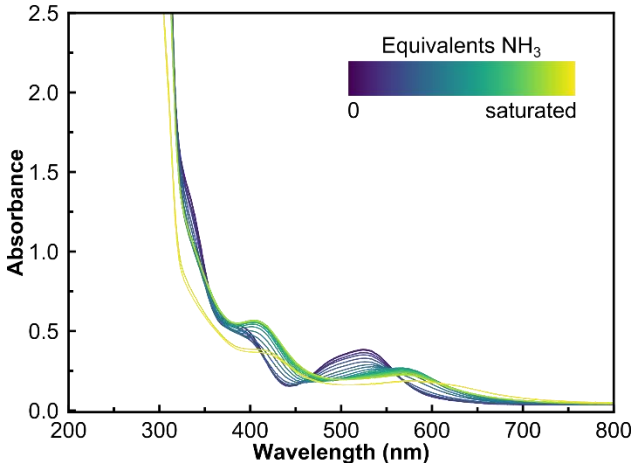

Figure D40. UV-vis spectra of acetonitrile solution containing 0.12 mM $[(BPM^{NMe2})Fe(MeCN)_2]OTf_2$ and varying equivalents NH_3 in a 1 cm cuvette.

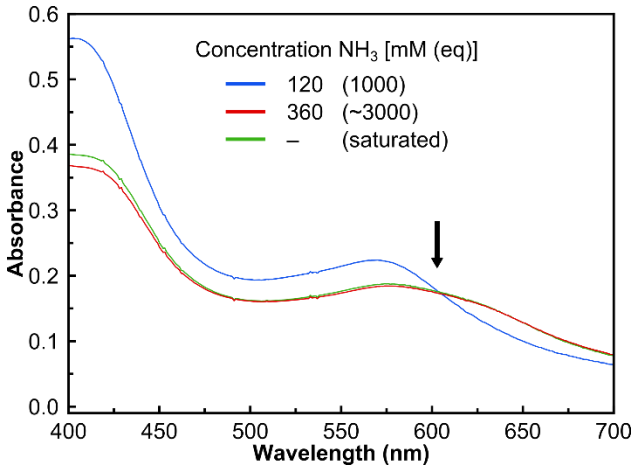

Figure D41. Selected UV-vis spectra used for determining the onset of demetallation for acetonitrile solution containing 0.12 mM $[(BPM^{NMe2})Fe(MeCN)_2]OTf_2$ and varying equivalents NH_3 in a 1 cm cuvette.

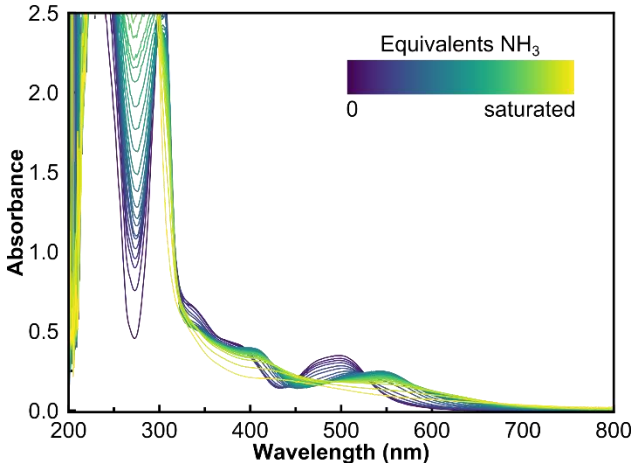

Figure D42. UV-vis spectra of acetonitrile solution containing 0.12 mM $[(BPM^{OMe})Fe(MeCN)_2]OTf_2$ and varying equivalents NH_3 in a 1 cm cuvette.

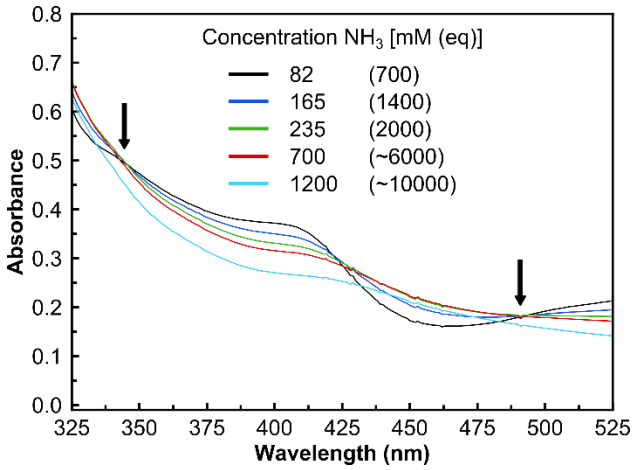

Figure D43. Selected UV-vis spectra used for determining the onset of demetallation for acetonitrile solution containing 0.12 mM $[(BPM^{OMe})Fe(MeCN)_2]OTf_2$ and varying equivalents NH_3 in a 1 cm cuvette.

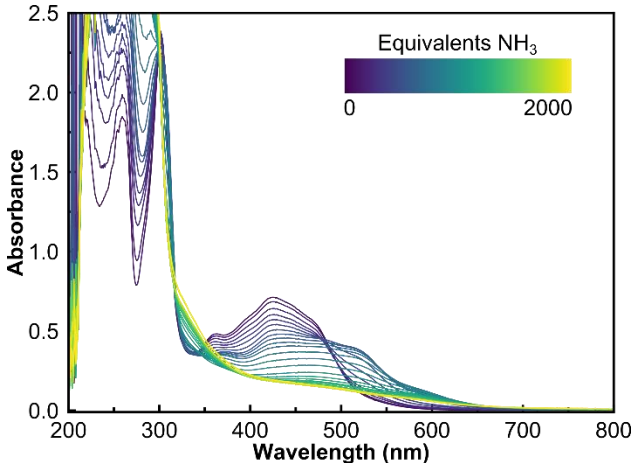

Figure D44. UV-vis spectra of acetonitrile solution containing 0.12 mM $[(BPM^{CF3})Fe(MeCN)_2]OTf_2$ and varying equivalents NH_3 in a 1 cm cuvette.

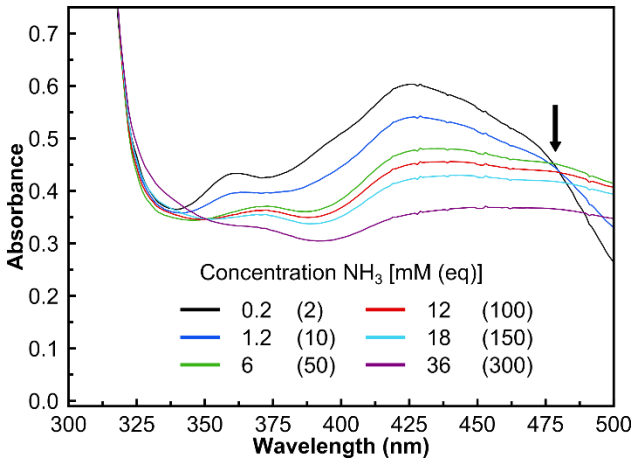

Figure D45. Selected UV-vis spectra used for determining the onset of demetallation for acetonitrile solution containing 0.12 mM $[(BPM^{CF3})Fe(MeCN)_2]OTf_2$ and varying equivalents NH_3 in a 1 cm cuvette.

D10. Mass spectrometry

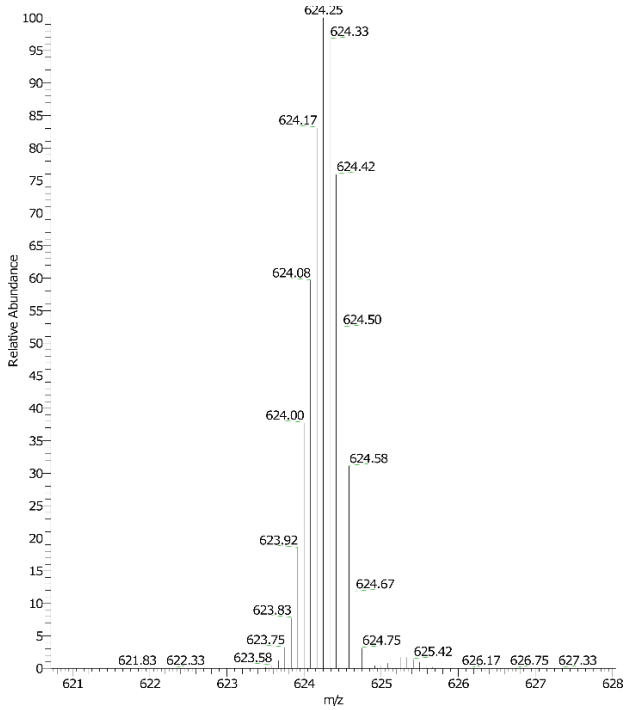

Figure D47. ESI mass spectrum of $[(TPA^{NMe2})Fe(MeCN)_2]OTf_2$ in acetonitrile.

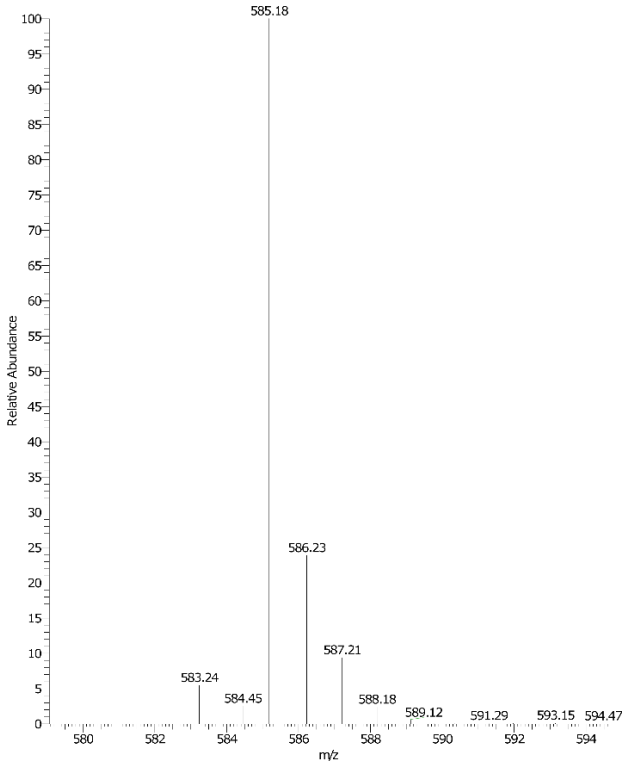

Figure D48. ESI mass spectrum of $[(TPA^{OMe})Fe(MeCN)_2]OTf_2$ in acetonitrile.

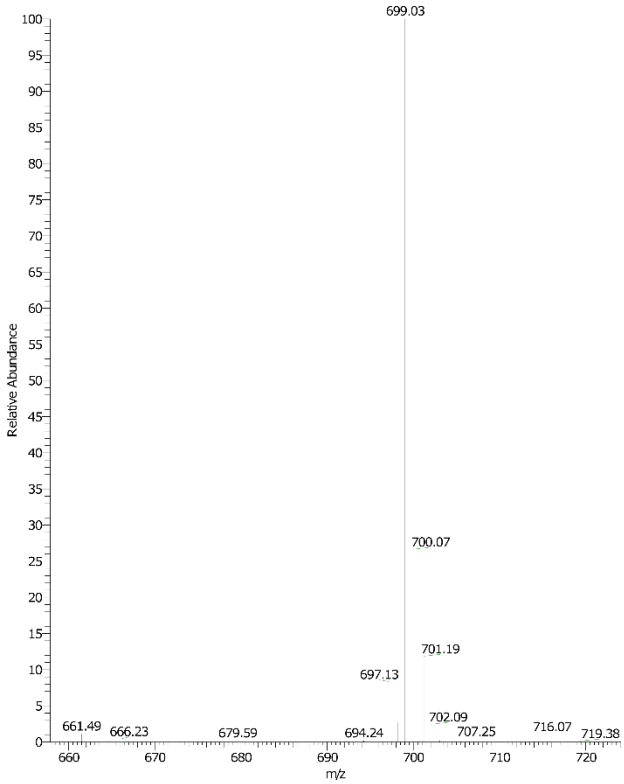

Figure D49. ESI mass spectrum of $[(TPA^{CF3})Fe(MeCN)_2]OTf_2$ in acetonitrile.

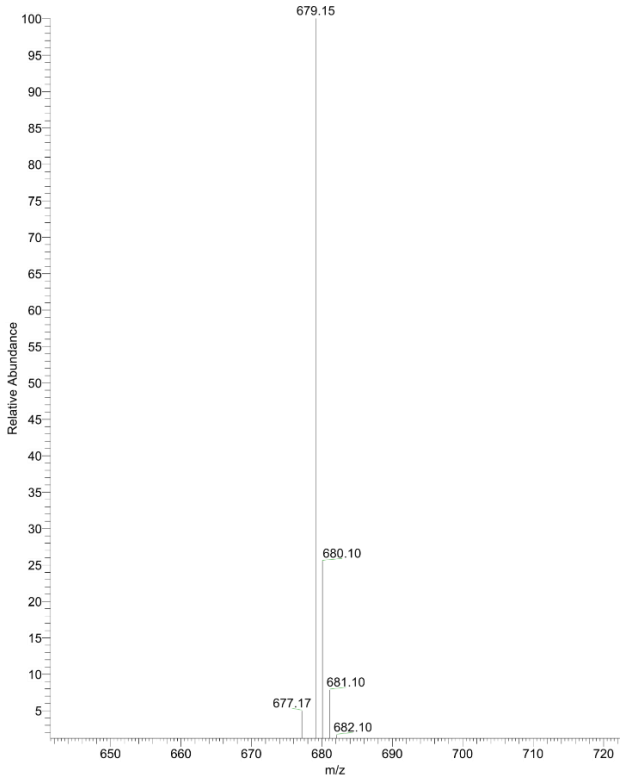

Figure D50. ESI mass spectrum of $[(BPM^{CF3})Fe(MeCN)_2]OTf_2$ in acetonitrile.

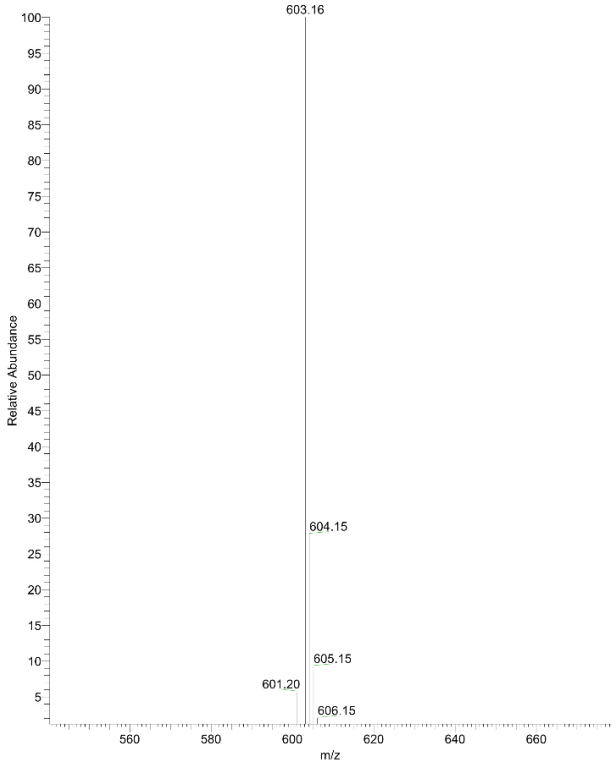

Figure D51. ESI mass spectrum of $[(BPM^{OMe})Fe(MeCN)_2]OTf_2$ in acetonitrile.

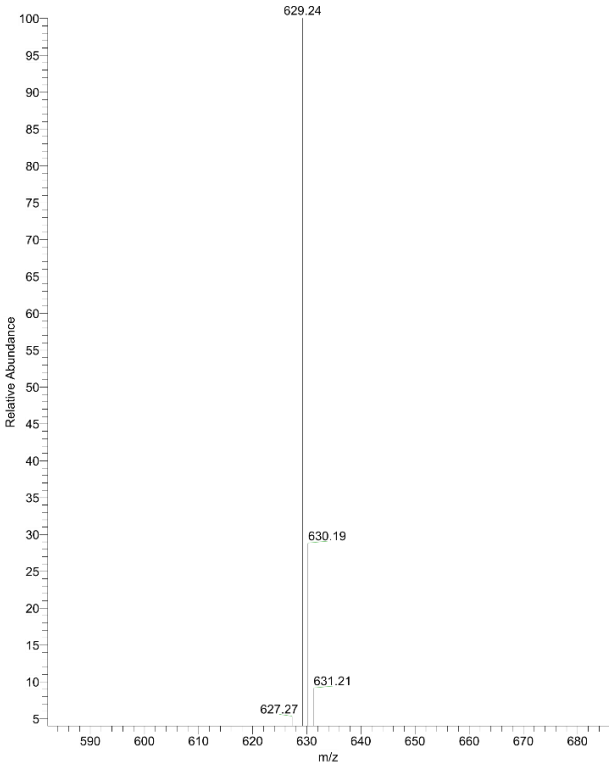

Figure D52. ESI mass spectrum of $[(BPM^{NMe2})Fe(MeCN)_2]OTf_2$ in acetonitrile.

D11. NMR spectra

TPA^{CF3} (tris(4-(trifluoromethyl)-2-picolyl)amine)

^{1}H NMR:

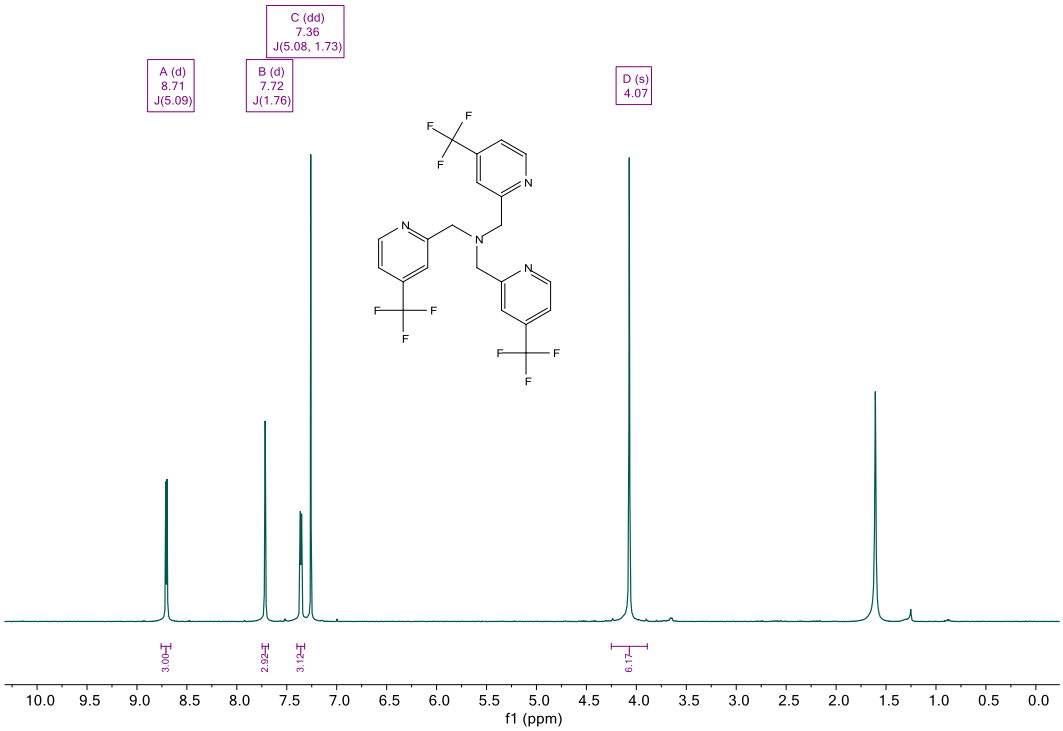

$^{13}C\{^{1}H\}$ NMR:

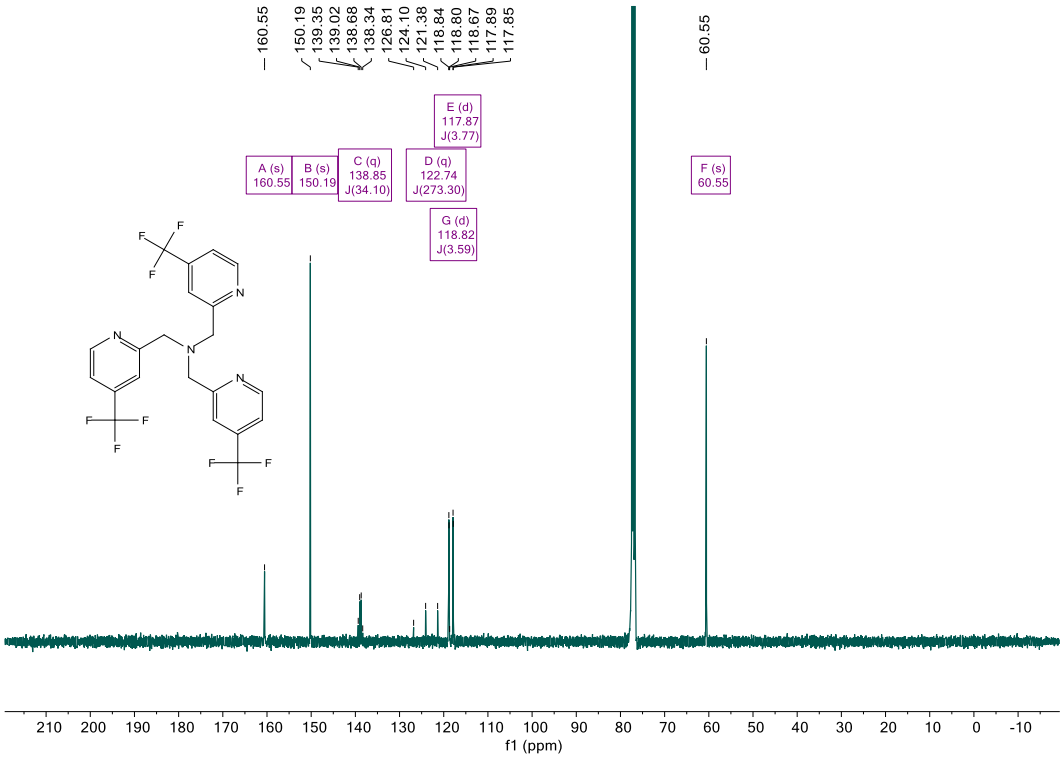

2,2'-(ethene-1,1-diyl)bis(4-(dimethylamino)pyridine)

^{1}H NMR:

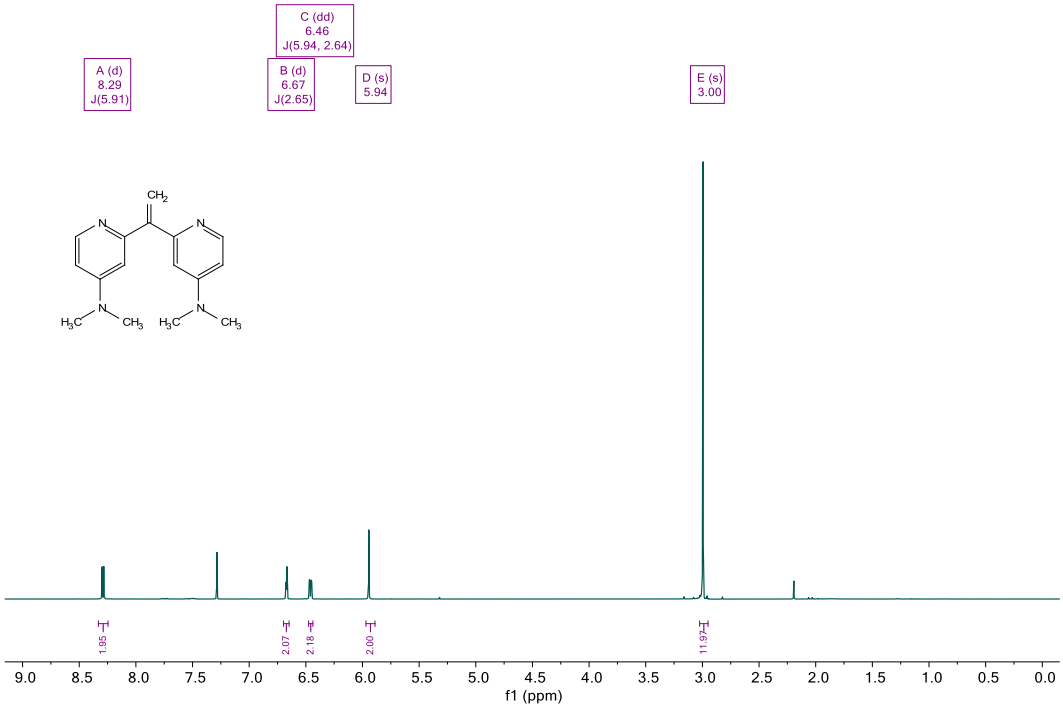

^{13}C{^{1}H} NMR:

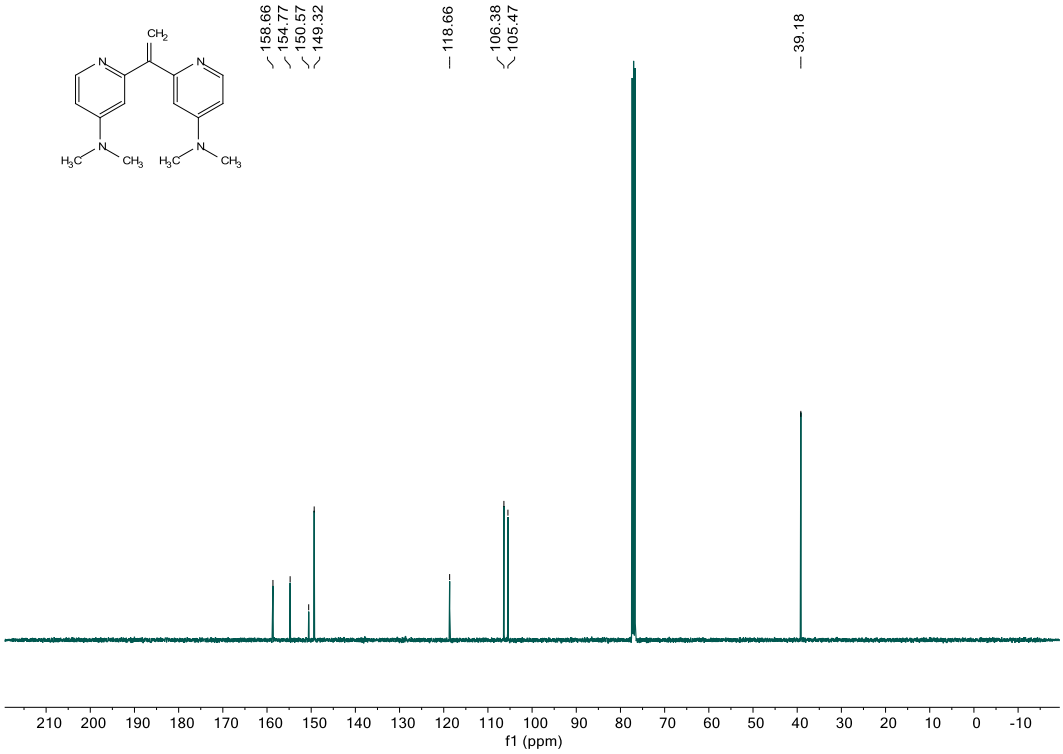

2,2'-(ethane-1,1-diyl)bis(4-(dimethylamino)pyridine)

^{1}H NMR:

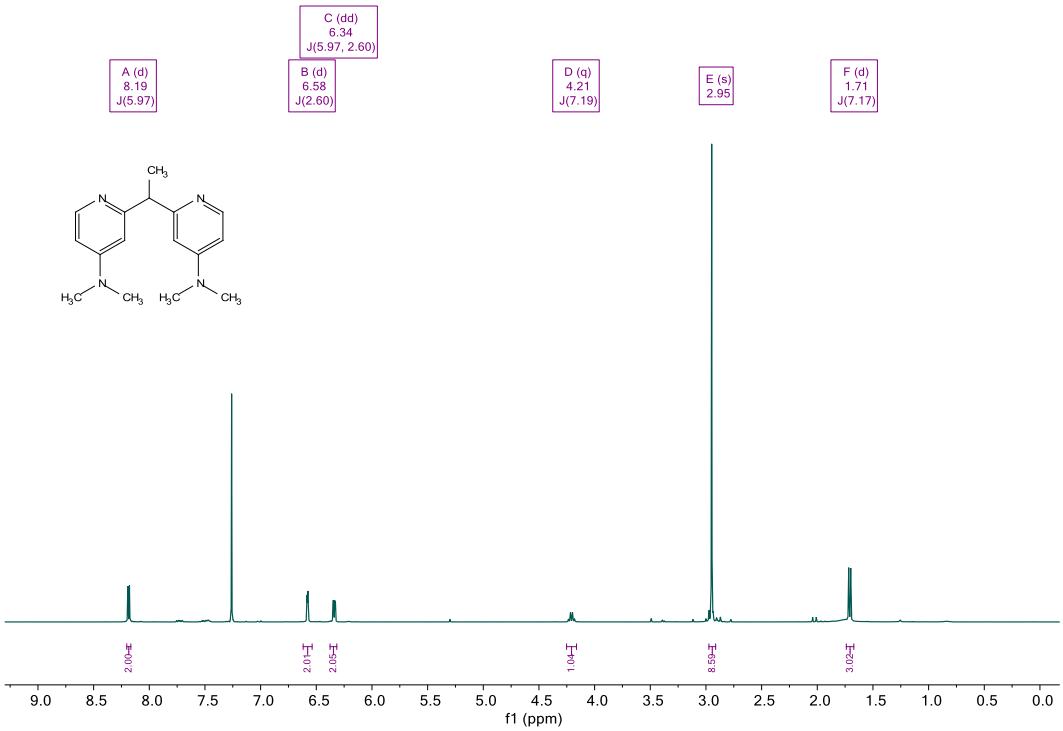

^{13}C{^{1}H} NMR:

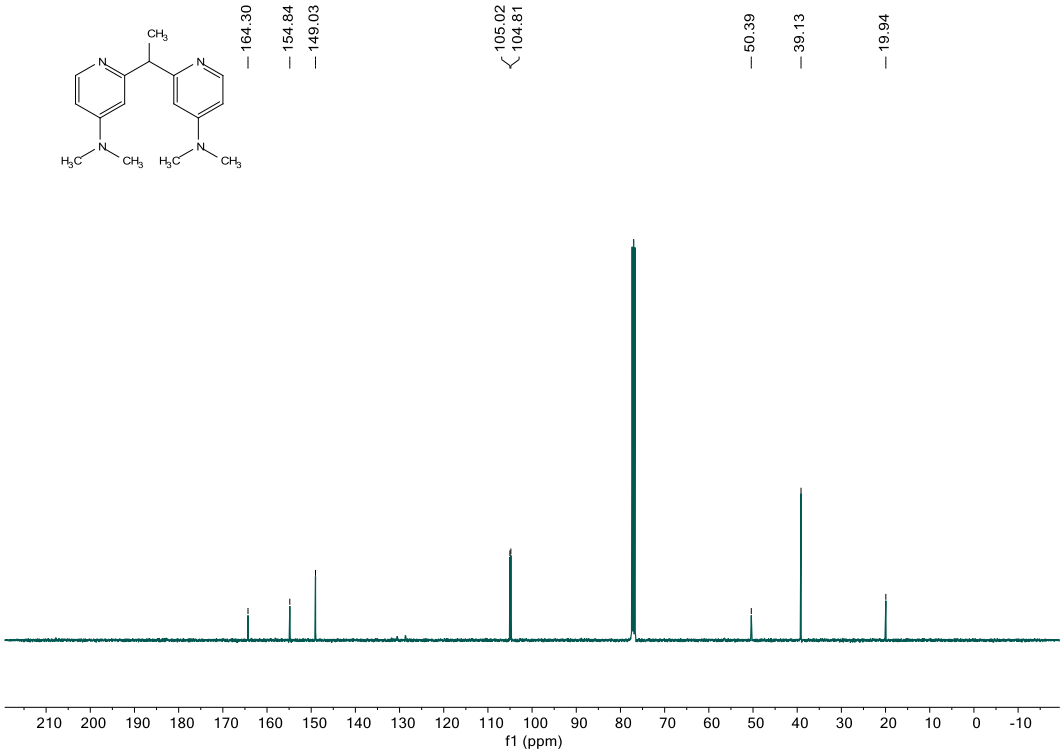

BPM^{NMe2} (6-(1,1-bis(4-(dimethylamino)pyridin-2-yl)ethyl)-2,2'-bipyridine)

^{1}H NMR:

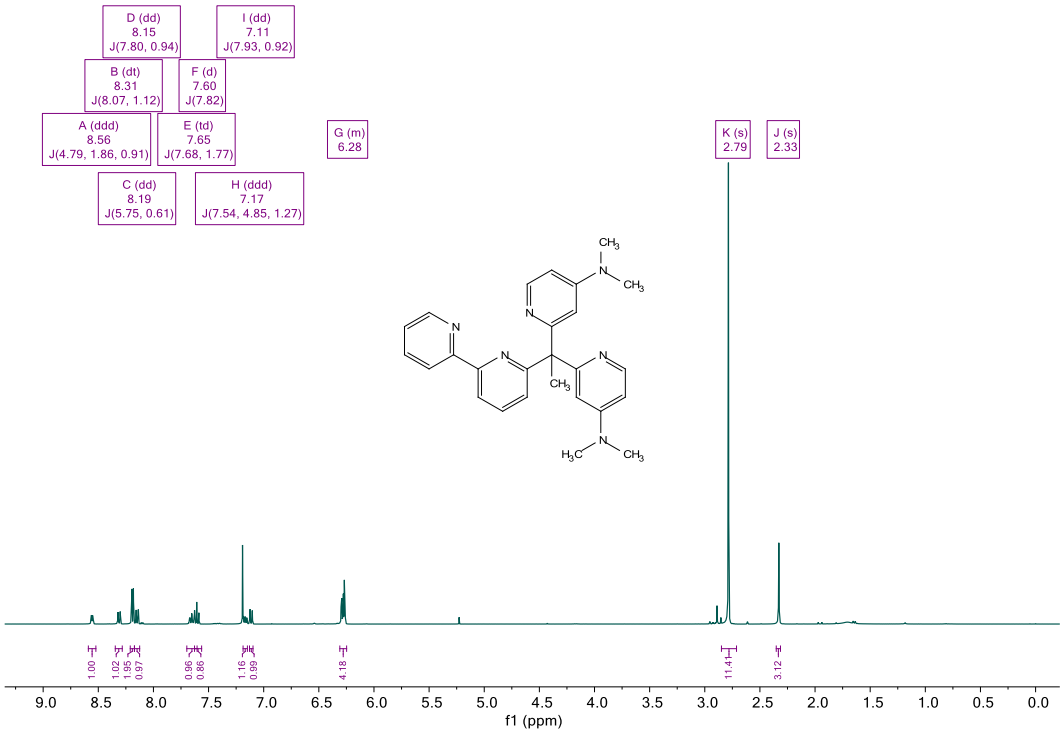

^{13}C{^{1}H} NMR:

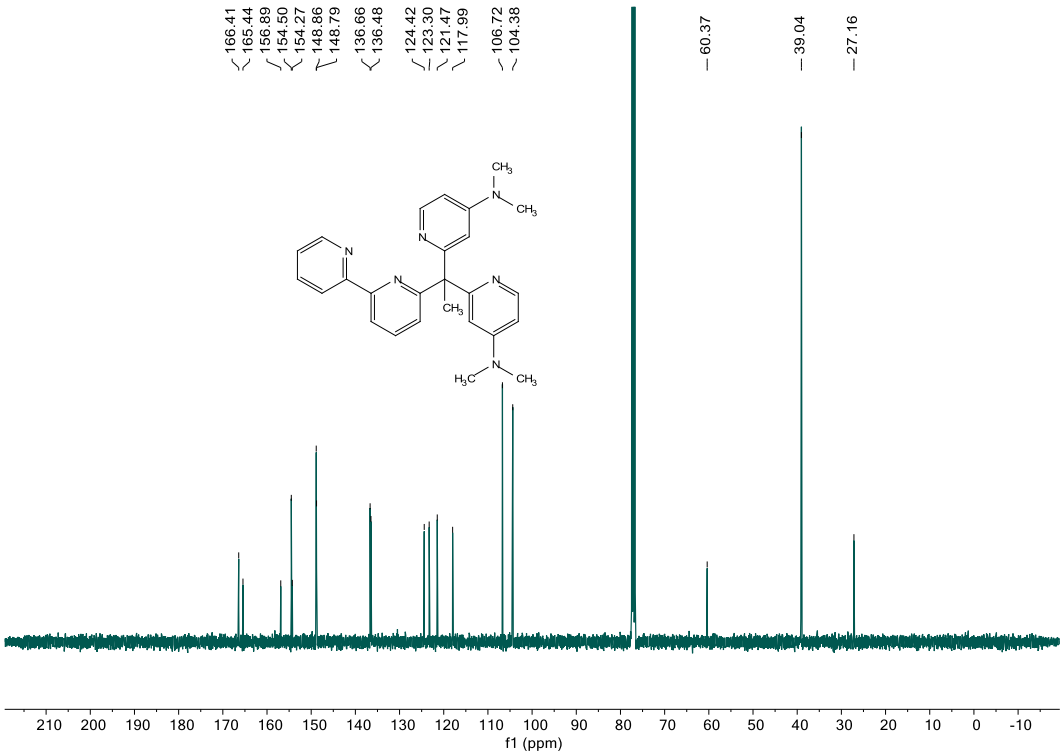

bis(4-methoxypyridin-2-yl)methanone

^{1}H NMR:

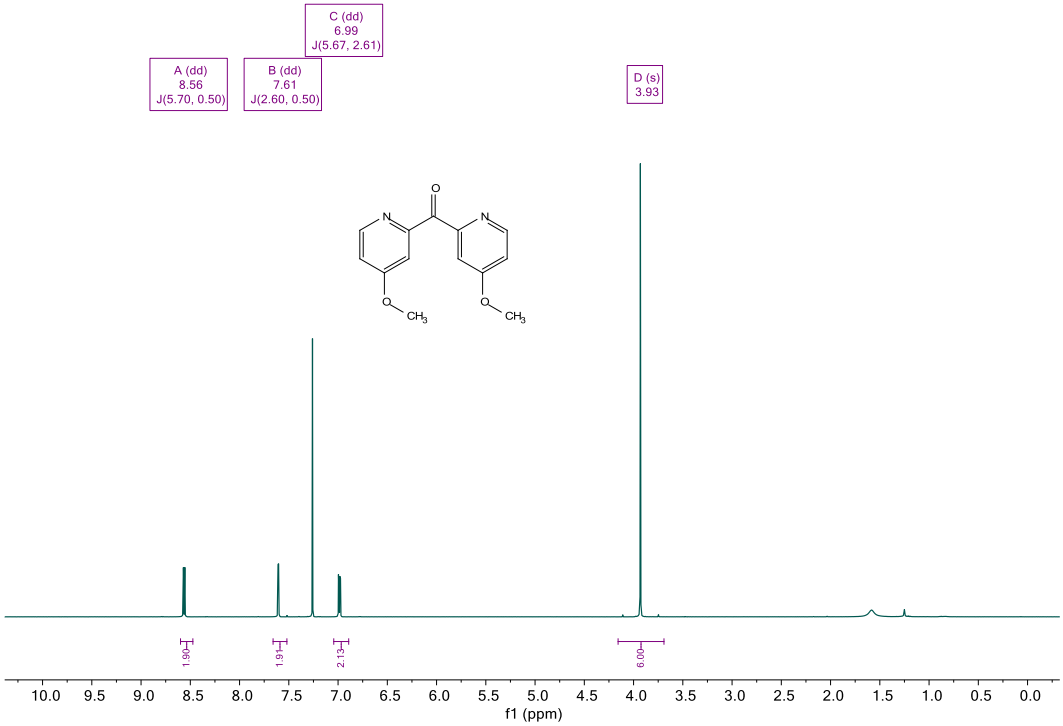

^{13}C{^{1}H} NMR:

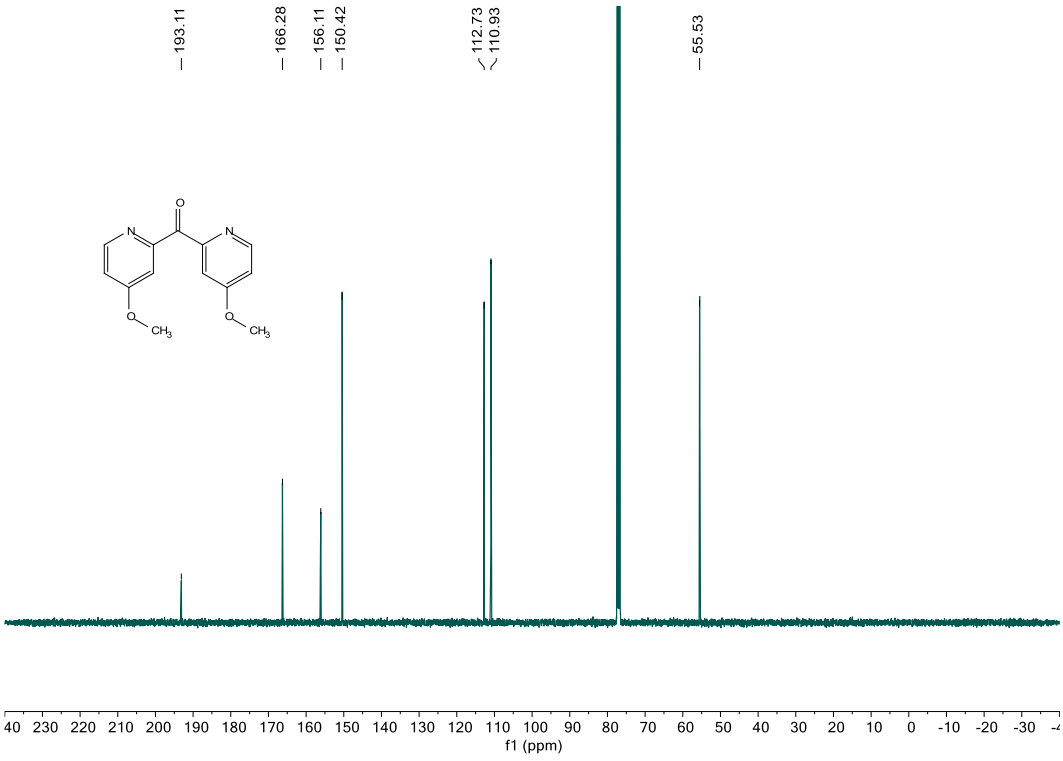

2,2'-(ethene-1,1-diyl)bis(4-(methoxypyridine)

^{1}H NMR:

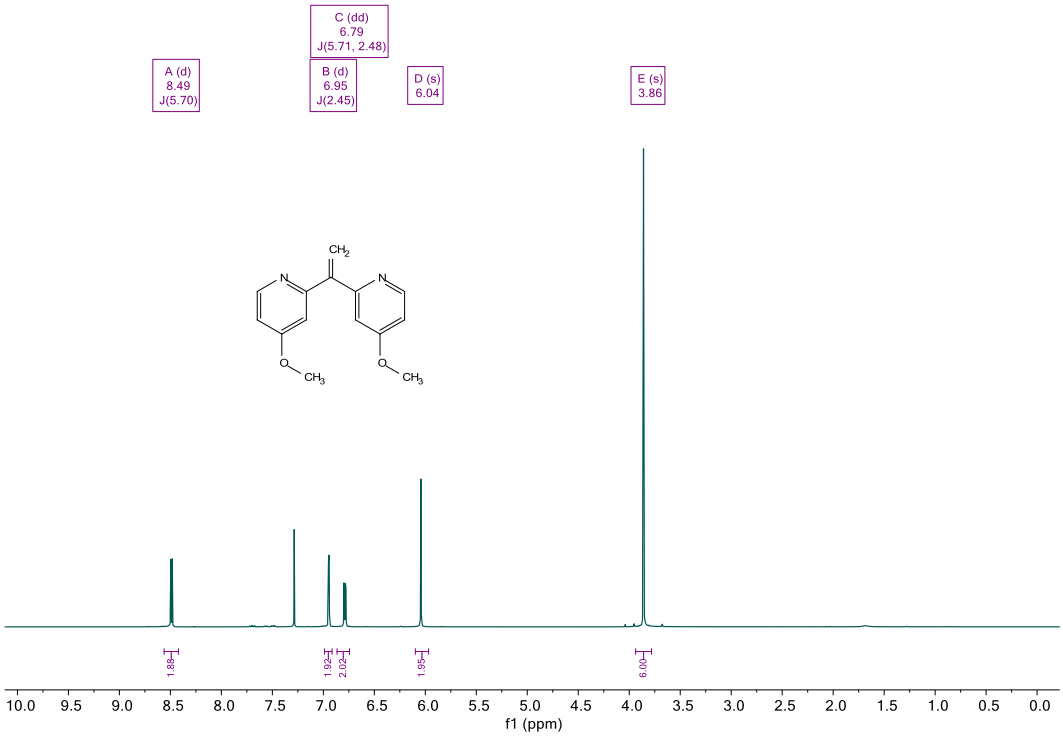

^{13}C{^{1}H} NMR:

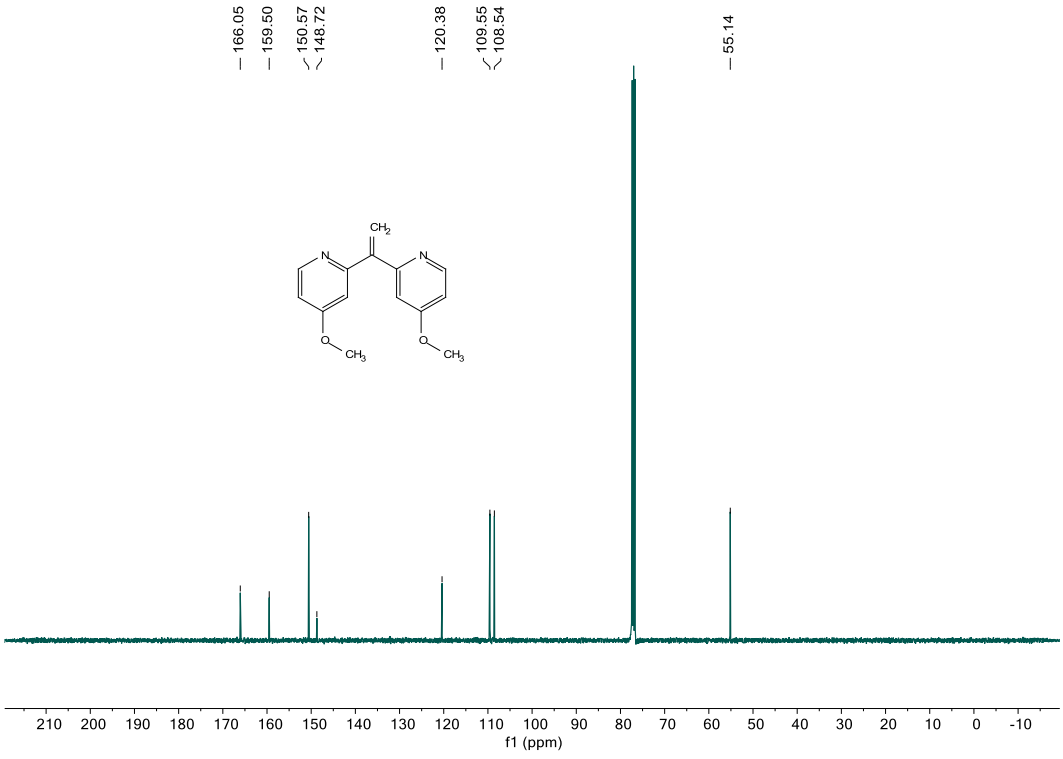

2,2'-(ethane-1,1-diyl)bis(4-methoxypyridine)

^{1}H NMR:

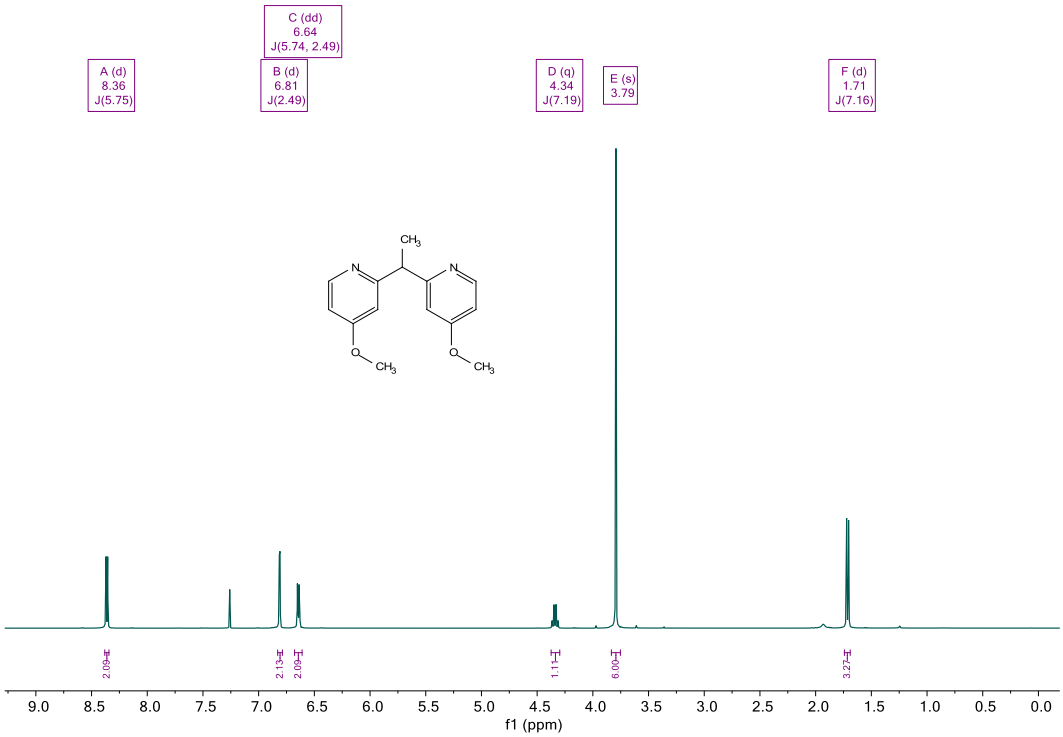

^{13}C{^{1}H} NMR:

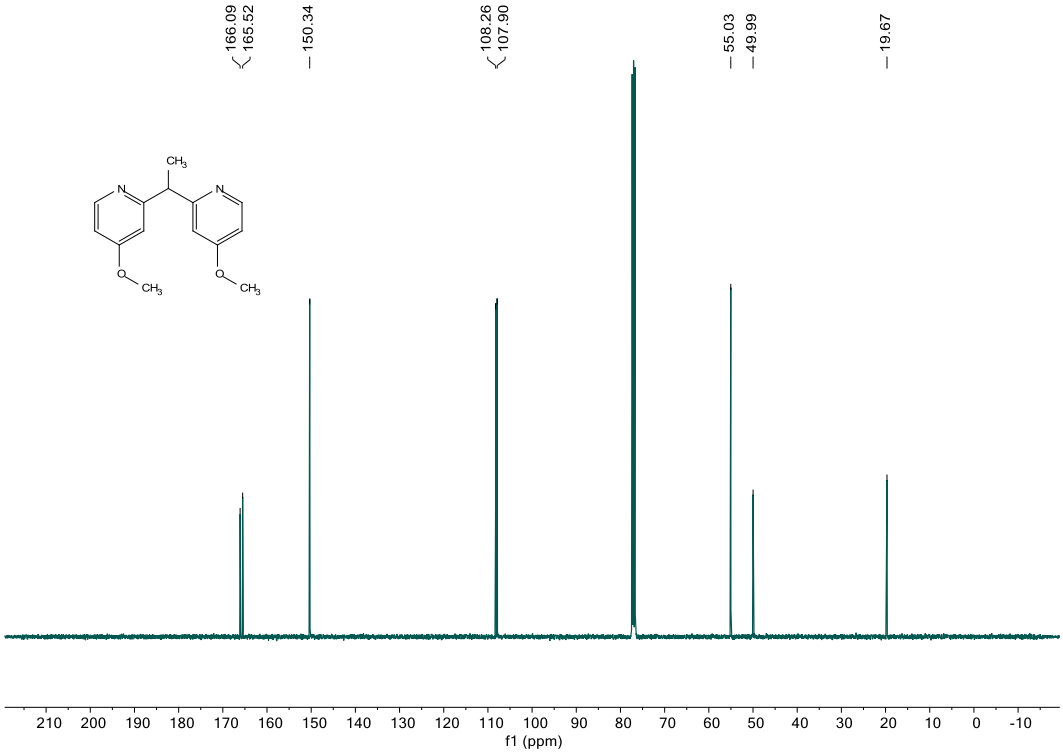

2,2',2'',2'''- 2,2',2'',2'''-(butane-1,1,3,3-tetrayl)tetrakis(4-methoxypyridine)

^{1}H NMR:

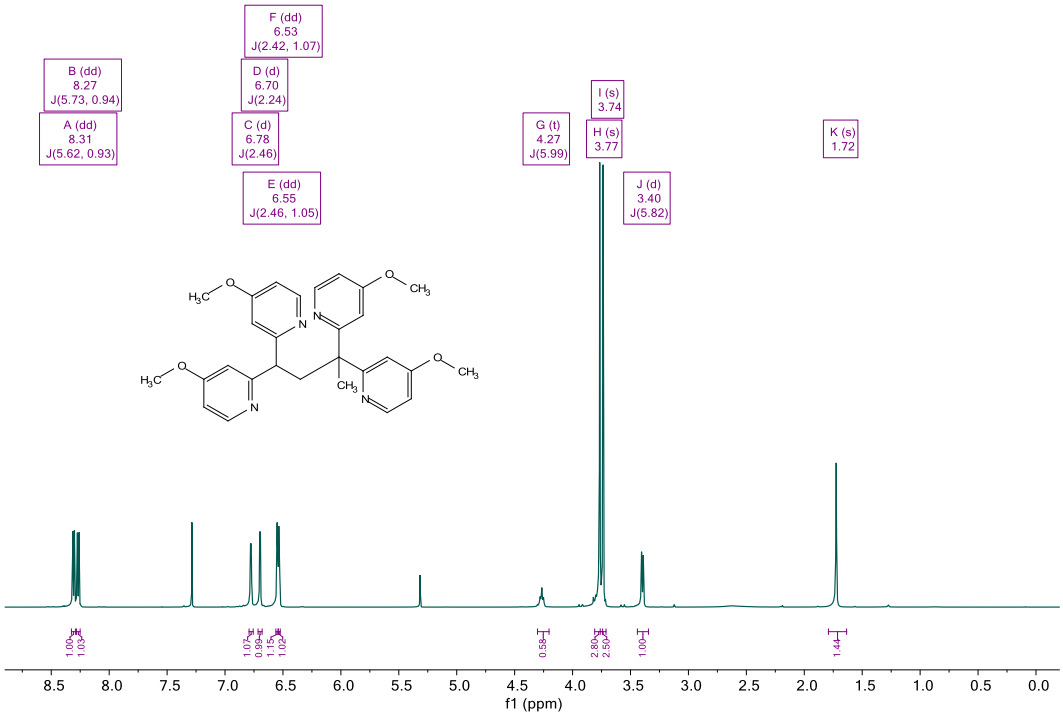

^{13}C{^{1}H} NMR:

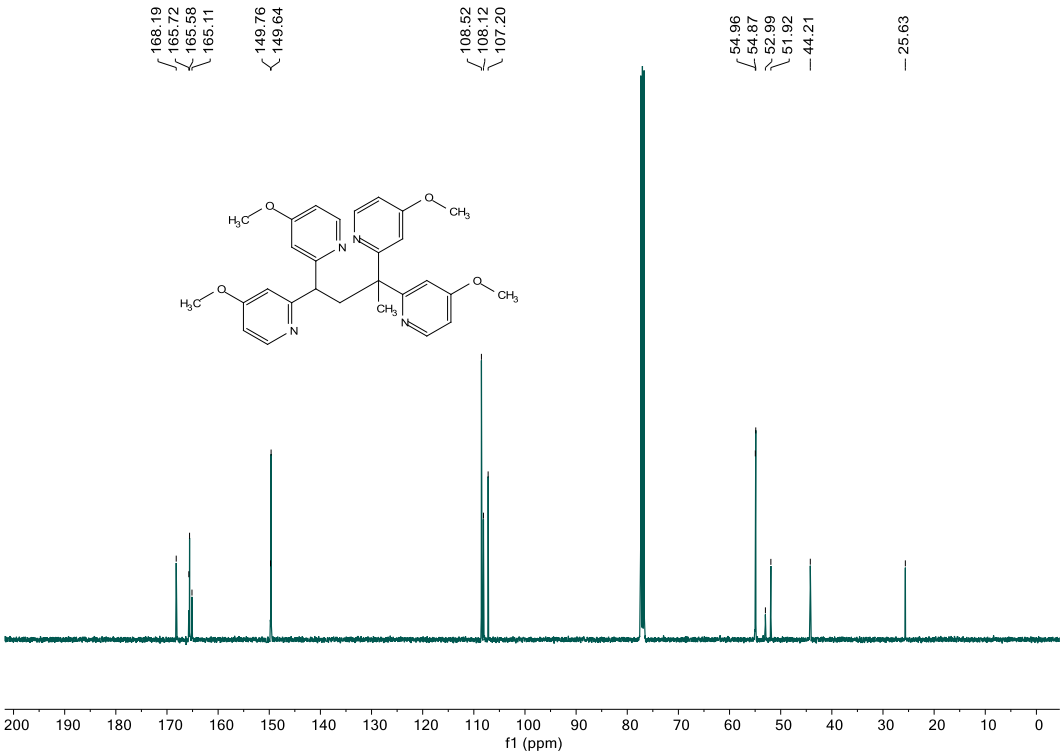

BPM^{OMe} (6-(1,1-bis(4-methoxypyridin-2-yl)ethyl)-2,2'-bipyridine)

^{1}H NMR:

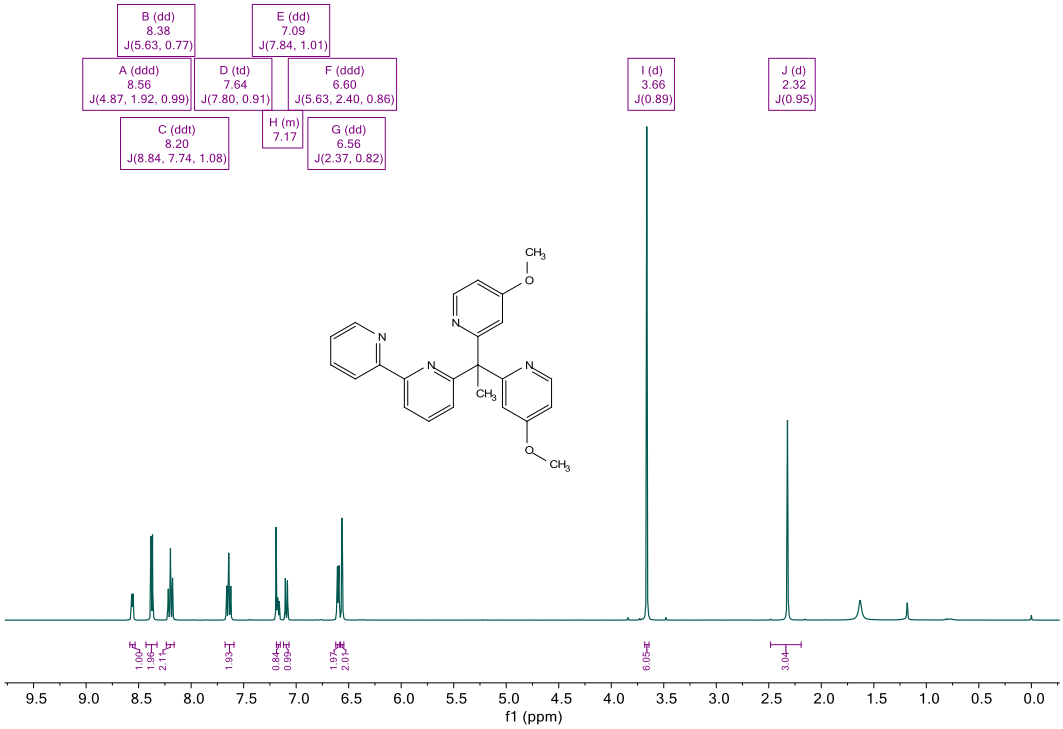

^{13}C{^{1}H} NMR:

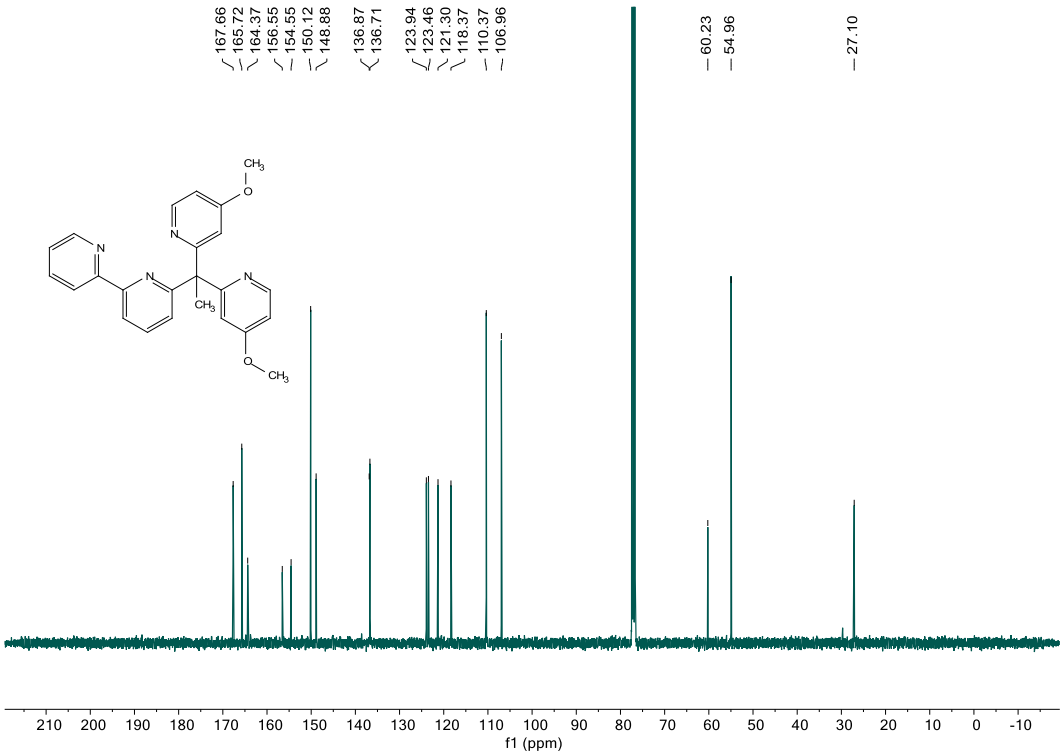

2,2'-(ethane-1,1-diyl)bis(4-(trifluoromethyl)pyridine)

^{1}H NMR:

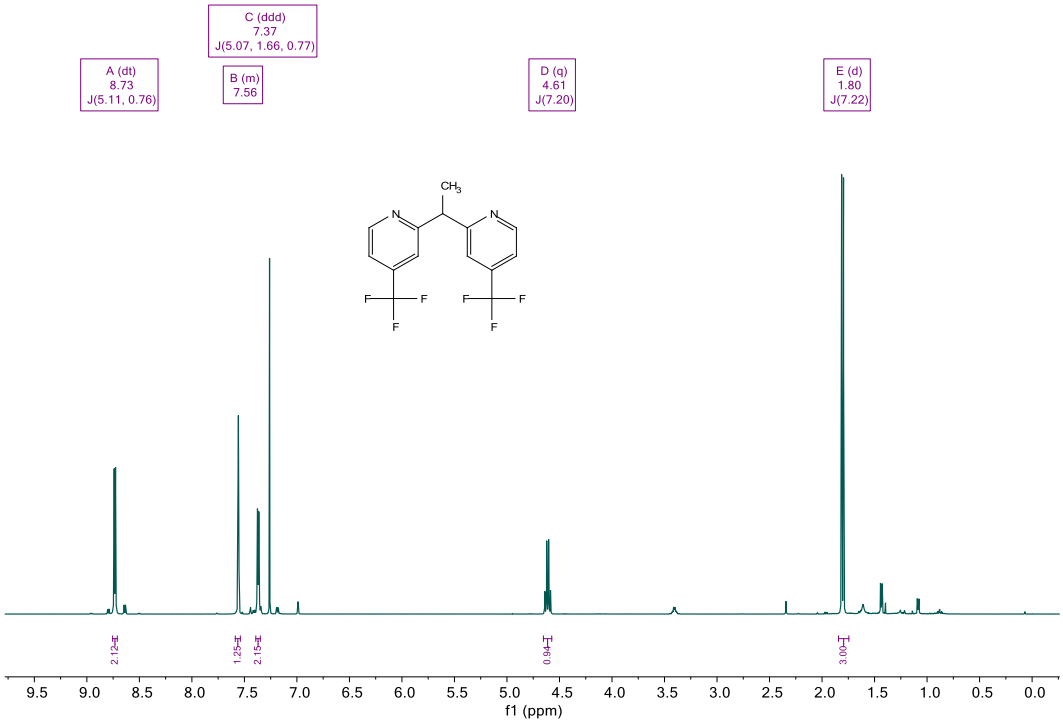

^{13}C{^{1}H} NMR:

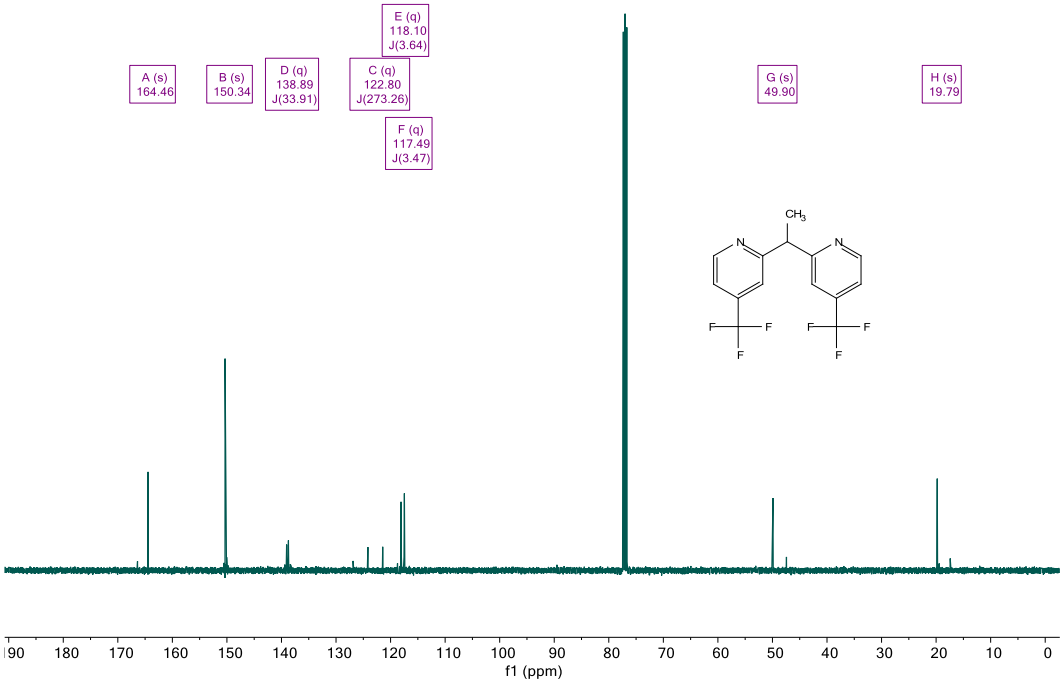

BPM^{CF3} (6-(1,1-bis(4-(trifluoromethyl)pyridin-2-yl)ethyl)-2,2'-bipyridine)

^{1}H NMR:

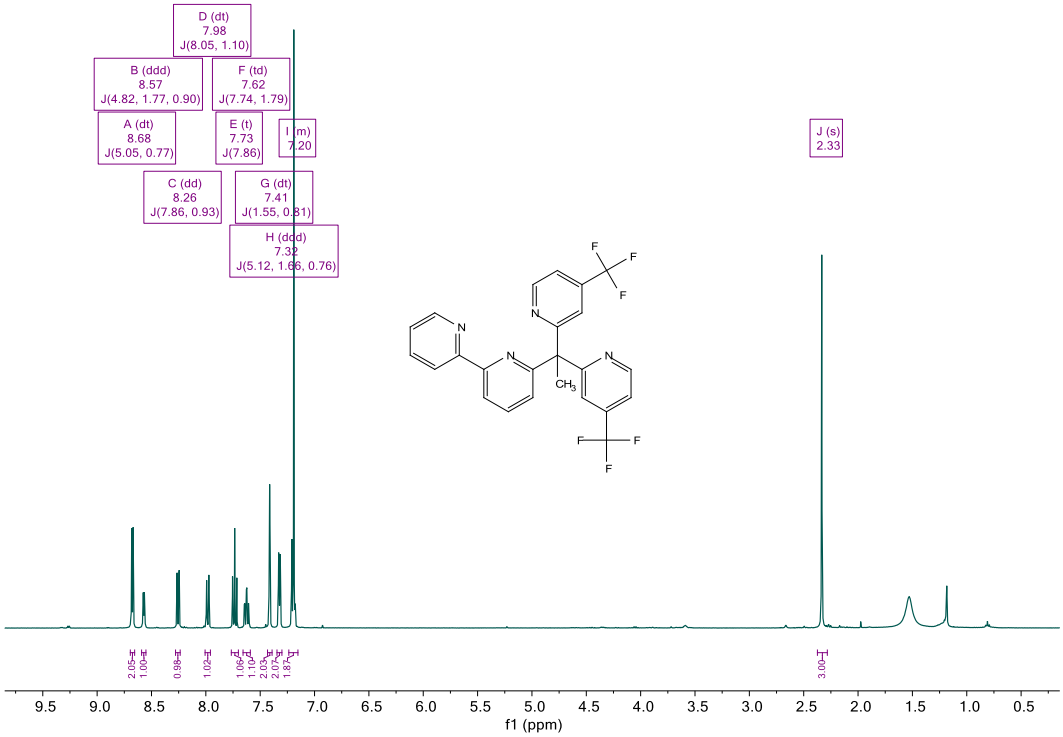

^{13}C{^{1}H} NMR:

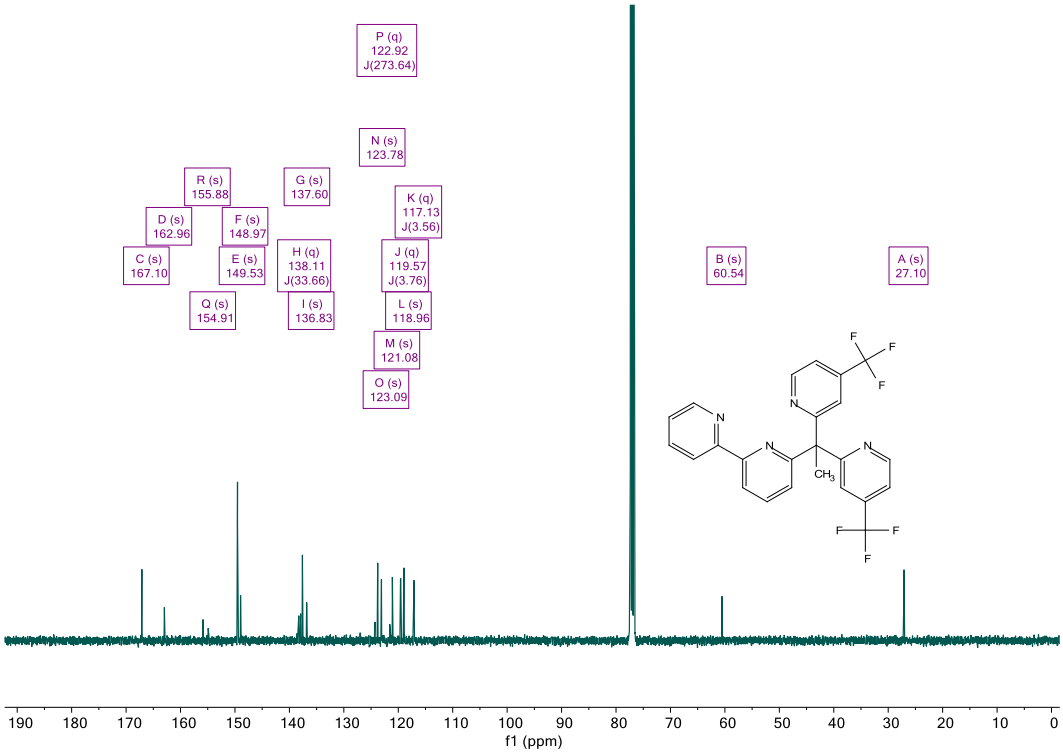

D.12 References

[1] Canary, J. W.; Wang, Y.; Roy, R. Tris[(2-pyridyl)methyl]amine (TPA) and (+)-bis[(2-pyridyl)methyl]-1-(2-pyridyl)-ethylamine (α-METPA). *Inorg. Synth.* **1998**, *32*, 70–75.

[2] Diebold, A.; Hagen, K. S. Iron(II) Polyamine Chemistry: Variation of Spin State and Coordination Number in Solid State and Solution with Iron(II) Tris(2-pyridylmethyl)amine Complexes. *Inorg. Chem.* **1998**, *37*, 215–223.

[3] Khnayzer, R. S.; Thoi, V. S.; Nippe, M.; King, A. E.; Jurss, J. W.; El Roz, K. A.; Long, J. R.; Chang, C. J.; Castellano, F. N. Towards a Comprehensive Understanding of Visible-Light Photogeneration of Hydrogen from Water Using Cobalt(II) Polypyridyl Catalysts. *Energy Environ. Sci.* **2014**, *7*, 1477–1488.

[4] Chen, L.; Su, X.-J.; Jurss, J. W. Selective Alkane C–H Bond Oxidation Catalyzed by a Non-Heme Iron Complex Featuring a Robust Tetradentate Ligand. *Organometallics* **2018**, *37*, 4535–4539.

[5] Miller, S. L.; Chotana, G. A.; Fritz, J. A.; Chattopadhyay, B.; Maleczka, R. E., Jr.; Smith, M. R., III. C–H Borylation Catalysts that Distinguish Between Similarly Sized Substituents Like Fluorine and Hydrogen. *Org. Lett.* **2019**, *21*, 6388–6392.

[6] Zhang, C. X.; Kaderli, S.; Costas, M.; Kim, E.; Neuhold, Y.; Karlin, K. D.; Zuberbühler, A. D. Copper(I)–Dioxygen Reactivity of $[(L)Cu^{I}]^{+}$ (L = Tris(2-Pyridylmethyl)amine): Kinetic/Thermodynamic and Spectroscopic Studies Concerning the Formation of $Cu–O_2$ and $Cu_2–O_2$ Adducts as a Function of Solvent Medium and 4-Pyridyl Ligand Substituent Variations. *Inorg. Chem.* **2003**, *42*, 1807–1824.

[7] Koide, K.; Bein, K.; Bressin, R.; Burrows, J.; Gambino, A.; Leikauf, G.; Pham, D. Analogs of 2-Pralidoxime as Antidotes Against Organophosphorus Nerve Agents. WO2020027905A2, February 6, 2020.

[8] Nippe, M.; Khnayzer, R. S.; Panetier, J. A.; Zee, D. Z.; Olaiya, B. S.; Head-Gordon, M.; Chang, C. J.; Castellano, F. N.; Long, J. R. Catalytic Proton Reduction with Transition Metal Complexes of the Redox-Active Ligand Bpy2PYMe. *Chem. Sci.* **2013**, *4*, 3934–3945.

[9] Miller, S. L.; Chotana, G. A.; Fritz, J. A.; Chattopadhyay, B.; Maleczka, R. E.; Smith, M. R. C–H Borylation Catalysts That Distinguish Between Similarly Sized Substituents Like Fluorine and Hydrogen. *Org. Lett.* **2019**, *21*, 6388–6392.

[10] Mu, X.; Axtell, J. C.; Bernier, N. A.; Kirlikovali, K. O.; Jung, D.; Umanzor, A.; Qian, K.; Chen, X.; Bay, K. L.; Kirollos, M.; Rheingold, A. L.; Houk, K. N.; Spokoyny, A. M. Sterically Unprotected Nucleophilic Boron Cluster Reagents. *Chem* **2019**, *5*, 2461–2469.

[11] Sheldrick, G. SHELXT - Integrated Space-Group and Crystal-Structure Determination. *Acta Crystallogr., Sect. C: Struct.* **2015**, *71*, 3–8.

[12] Dolomanov, O. V.; Bourhis, L. J.; Gildea, R. J.; Howard, J. A. K.; Puschmann, H. OLEX2: a Complete Structure Solution, Refinement and Analysis Program. *J. Appl. Crystallogr.* **2009**, *42*, 339–341.

[13] Subramanyam, C. An Unusual Dependency of Counterion During Wittig Methylenation of Bis-Heteroaryl Ketones. *Tetrahedron Lett.* **1995**, *36*, 9249–9252.

[14] Bechlars, B.; D'Alessandro, D. M.; Jenkins, D. M.; Iavarone, A. T.; Glover, S. D.; Kubiak, C. P.; Long, J. R. High-Spin Ground States via Electron Delocalization in Mixed-Valence Imidazolate-Bridged Divanadium Complexes. *Nat. Chem.* **2010**, *2*, 362–368.

[15] Macpherson, J. V. A Practical Guide to Using Boron Doped Diamond in Electrochemical Research. *Phys. Chem. Chem. Phys.* **2015**, *17*, 2935–2949.

[16] Lindley, B. M.; Appel, A. M.; Krogh-Jespersen, K.; Mayer, J. M.; Miller, A. J. M. Evaluating the Thermodynamics of Electrocatalytic N_2 Reduction in Acetonitrile. *ACS Energy Lett.* **2016,** *1*, 698–704.